Scientific Research Publishing

Open Journal of Applied Sciences, 2026, 16(10), 4093-4122
https://www.scirp.org/journal/ojapps
ISSN Online: 2165-3925
ISSN Print: 2165-3917

Co-Design of Periodic Event-Triggered Quantization Control for Linear Systems with Packet Losses

Mengfan Hou

School of Mathematics and Statistics, North China University of Water Resources and Electric Power, Zhengzhou, China
Email: houmf2259@163.com

How to cite this paper: Hou, M.F. (2026) Co-Design of Periodic Event-Triggered Quantization Control for Linear Systems with Packet Losses. *Open Journal of Applied Sciences*, **16**, 4093-4122.
https://doi.org/10.4236/ojapps.2026.1610225

Received: September 11, 2026
Accepted: October 27, 2026
Published: October 30, 2026

Copyright © 2026 by author(s) and Scientific Research Publishing Inc.
This work is licensed under the Creative Commons Attribution International License (CC BY 4.0).
http://creativecommons.org/licenses/by/4.0/

Open Access

Abstract

This paper investigates the co-design problem of an event-triggered communication mechanism and a dynamic output feedback controller for networked control systems (NCSs) subject to packet losses and quantization errors under a no-ACK transmission mechanism. For the baseline scenario with packet losses only, an augmented closed-loop system model incorporating registers and auxiliary variables is constructed to characterize the effects of consecutive packet losses. A Lyapunov-based approach is then employed to derive sufficient linear matrix inequality (LMI) conditions for $\mathcal{L}_2$-stability, based on which the dynamic periodic event-triggered mechanism (PETM) and the dynamic output feedback controller are co-designed. To further account for quantized signal transmission, a dynamic quantization scheme is introduced to prevent quantizer saturation caused by external disturbances through adaptive adjustment of the quantization scaling parameter. The dynamic PETM and dynamic quantizer are jointly designed as a unified dynamic periodic event-triggered quantization mechanism (PETQM), based on which an augmented closed-loop system model is established. The LMI conditions derived for the baseline scenario are then employed to facilitate the joint design of the dynamic PETQM and the dynamic output feedback controller, while accounting for the coupled effects of packet losses and quantization errors. Numerical examples demonstrate that the proposed method reduces network transmissions while maintaining the stability and control performance of the closed-loop system.

Keywords

Periodic Event-Triggered Mechanism (PETM), Dynamic Output Feedback Control, Packet Losses, Dynamic Quantizer, Linear Matrix Inequalities (LMIs)

1. Introduction

Networked control systems (NCSs) are feedback control systems in which sensors, controllers, actuators, and plants communicate with each other through digital communication networks [1] [2]. Benefiting from their inherent advantages of flexible deployment, reduced wiring, and convenient maintenance, NCSs are widely used in industrial automation [3], intelligent transportation systems [4], and smart grids [5]. However, communication in NCSs relies on open digital networks and is inevitably subject to imperfections such as packet losses and bandwidth limitations. These phenomena often interact, significantly degrading system performance and potentially destabilizing the closed-loop system if not properly handled. Consequently, developing strategies that can simultaneously guarantee satisfactory control performance and efficient communication resource utilization has become a critical research challenge.

To reduce unnecessary communication, event-triggered control (ETC) was proposed to transmit data only when necessary in [6] [7]. Most existing studies consider continuous ETC (CETC), where the triggering condition is continuously evaluated [5] [8]-[10]. However, continuous evaluation makes it difficult to guarantee a positive minimum inter-event time (MIET), which may lead to the Zeno phenomenon. In contrast, periodic ETC (PETC) evaluates the triggering condition only at discrete sampling instants [11]. The sampling period thus provides a positive MIET and naturally excludes Zeno behavior. Moreover, [12] showed that dynamic ETC can reduce the number of communication events. By introducing additional dynamic variables, dynamic periodic event-triggered mechanism (PETM) provides greater flexibility in designing the triggering conditions [13]-[16]. These advantages motivate the study of dynamic PETMs in this paper.

Due to the unreliability of network transmission, packet loss is an unavoidable phenomenon in NCSs, which may degrade system performance or even destabilize the closed-loop system [9]. To address the effects of packet losses, various packet loss models have been considered in the literature. For example, random packet losses have been investigated in [17] [18], while consecutive packet losses have been considered in [10] [15] [19]. It should be noted that the studies in [10] [15] [19] rely on acknowledgment mechanisms or assume that acknowledgment signals are transmitted without delay. However, in practical NCSs, acknowledgment signals may also experience packet losses or transmission delays during network transmission. Therefore, some recent studies, such as [9] [16], have investigated NCSs subject to packet losses without acknowledgment (no-ACK) mechanisms. In this paper, the baseline NCS considers consecutive packet losses under the no-ACK mechanisms.

In addition to packet loss, the inherent bandwidth limitations of communication networks necessitate the quantization of signals prior to transmission. A quantizer is a mapping that maps a signal from a continuous-valued domain to a finite set of discrete values. Existing quantization strategies are generally divided into static quantization [20] [21] and dynamic quantization [22]-[25]. Since the error

bound of a static quantizer (SQ) is fixed, an infinite quantization range is often assumed to avoid saturation when the signal exceeds the quantization range. However, an infinite quantization range is difficult to realize in practice [21]. To overcome this limitation, [22] proposed a scaling-factor-based approach that dynamically adjusts the quantizer range and the quantizer error bound. However, most existing studies have not simultaneously considered consecutive packet losses and dynamic quantization in the absence of an acknowledgment mechanism. Motivated by these developments, this paper further investigates the effects of consecutive packet losses and quantization errors on closed-loop systems without an acknowledgment mechanism.

Most existing studies adopt a simulation-based design approach, where the controller is first designed without considering the network, followed by the design of an event triggering strategy for the resulting closed-loop system [10] [23] [24]. However, such a design procedure does not adequately capture the coupling between network constraints and controller synthesis. Consequently, the controller and event triggering mechanism may not be well coordinated, making it difficult to guarantee the stability of the resulting NCS. To address this issue, the co-design of event-triggering strategies and controllers has attracted increasing attention, as demonstrated in [26]-[29].

This paper considers two related co-design problems for NCSs under packet losses in the no-ACK network environment. First, dynamic PETMs for the sensor-to-controller and controller-to-actuator channels are co-designed with a dynamic output feedback controller for the baseline NCS with packet losses. An augmented closed-loop system model is constructed by introducing registers and auxiliary variables, based on which sufficient conditions for $\mathcal{L}_2$ stability are derived in the form of LMIs. Second, the framework is extended to NCSs subject to both packet losses and quantization errors by introducing dynamic quantizers. The scaling variables of the dynamic quantizers are adjusted dynamically to avoid saturation caused by external disturbances, while the dynamic quantizers enable finite-bit transmission at each transmission instant. The quantization errors are further incorporated into the event triggering conditions, leading to a co-design method for the dynamic PETQMs and controller that guarantees $\mathcal{L}_2$ stability of the resulting closed-loop system. The designed PETMs and PETQMs can be implemented using only locally available information at the triggering mechanisms, without relying on acknowledgment signals.

The remainder of this paper is organized as follows. Section 2 presents the problem formulation and introduces the two network environments considered in this paper. Section 3 addresses the co-design of dynamic PETMs and a dynamic output feedback controller for the baseline NCS under no-ACK packet losses. The closed-loop system model is first established, followed by the derivation of sufficient conditions for $\mathcal{L}_2$ stability. Section 4 extends the framework by incorporating dynamic quantization. The parameters of the dynamic quantizers are first designed, after which the closed-loop system model under the dynamic PETQM is estab-

lished and its $\mathcal{L}_2$ stability is analyzed. Section 5 verifies the effectiveness of the proposed approaches via a numerical example. Finally, Section 6 concludes the paper.

Notations: $\mathbb{R}^n$ denotes the n-dimensional Euclidean space and $\mathbb{N}$ denotes the set of nonnegative integers. Denote $\mathbb{N}_{>0}=\mathbb{N}\setminus\{0\}$, $\mathbb{R}_{\geq 0}=[0,\infty)$ and $\mathbb{R}_{>0}=(0,\infty)$. $\mathbf{0}$ and I_n stand for the zero matrix of appropriate dimensions and the n-dimensional identity matrix, respectively. For vectors $x_i\in\mathbb{R}^{n_{x_i}}$, $i\in\{1,2,\cdots,M\}$, $(x_1,x_2,\cdots,x_M)$ stands for $\left[x_1^{\mathrm{T}},x_2^{\mathrm{T}},\cdots,x_M^{\mathrm{T}}\right]^{\mathrm{T}}$. The maximum and minimum eigenvalues of a symmetric matrix A are denoted by $\lambda_{\min}(A)$ and $\lambda_{\max}(A)$, respectively. A continuous function $\alpha:\mathbb{R}_{\geq 0}\to\mathbb{R}_{\geq 0}$ is referred to as the class-$\mathcal{K}$ function if it is strictly increasing and satisfies $\alpha(0)=0$. Furthermore, if the function is of class $\mathcal{K}$ and unbounded, it is said to be the class-$\mathcal{K}_\infty$ function. A function $g:D\subset\mathbb{R}^n\to\mathbb{R}^n$ is said to be locally Lipschitz function if there exists a positive constant $K\in\mathbb{R}_{>0}$ satisfying $|g(a)-g(b)|\leq K|a-b|$, for $\forall a,b\in D$, where K is said to be the Lipschitz constant. For a real number a, we denote $\lfloor a\rfloor$ as the nearest integer to a, *i.e.*, $\lfloor a\rfloor:=\min\{n\in\mathbb{N}\mid a\leq n\}$. For $x\in\mathbb{R}^n$ and a locally Lipschitz function $U:\mathbb{R}^n\to\mathbb{R}$, $U^\circ(x;v)$ is the Clarke derivative of the function U at x in the direction v, *i.e.*,

$$U^\circ(x;v)=\limsup_{y\to x,\lambda\downarrow 0}\frac{U(y+\lambda v)-U(y)}{\lambda}.$$

2. Problem Formulation

Consider the following linear time-invariant plant:

$$\begin{cases}\dot{x}_p(t)=A_p x_p(t)+B_p\hat{u}(t)+E_p\omega(t),\\ y(t)=C_p x_p(t),\end{cases}\tag{1}$$

where $x_p(t)\in\mathbb{R}^{n_{x_p}}$ is the state of plant, $\hat{u}(t)\in\mathbb{R}^{n_u}$ is the most recent control input available at the actuator, $\omega(t)\in\mathbb{R}^{n_\omega}$ is an exogenous disturbance, $y(t)\in\mathbb{R}^{n_y}$ is the measurement output, A_p, B_p, E_p and C_p are known matrices with appropriate dimensions. The dynamic output feedback controller is given in the following form

$$\begin{cases}\dot{x}_c(t)=A_c x_c(t)+B_c\hat{y}(t),\\ u(t)=C_c x_c(t),\end{cases}\tag{2}$$

where $x_c(t)\in\mathbb{R}^{n_{x_c}}$ is the controller state, $\hat{y}(t)\in\mathbb{R}^{n_y}$ is the most recently received measured output by the controller, and $A_c\in\mathbb{R}^{n_{x_c}\times n_{x_c}}$, $B_c\in\mathbb{R}^{n_{x_c}\times n_y}$ and $C_c\in\mathbb{R}^{n_u\times n_{x_c}}$ are matrices to be designed. The performance output is given by

$$z(t)=C_z x(t),\tag{3}$$

where $z(t)\in\mathbb{R}^{n_z}$, $x=(x_p,x_c)$ with $n_x:=n_{x_p}+n_{x_c}$, and $C_z=\begin{bmatrix}C_{zp} & 0\end{bmatrix}\in\mathbb{R}^{n_z\times n_x}$. Note that $\hat{y}$ and $\hat{u}$ denote the networked versions of y and u, respectively. Define the augmented vector $v=(y,u)\in\mathbb{R}^{n_v}$, where $v_1=y\in\mathbb{R}^{n_y}$, $v_2=u\in\mathbb{R}^{n_u}$, and $n_v=n_y+n_u$. The network-induced error is then defined as $e:=\hat{v}-v$, where

$e=(e_1,e_2)$, $e_1=:\hat{y}-y$ and $e_2=:\hat{u}-u$.

2.1. Network Environment

This section describes the communication environment and signal transmission mechanism considered in this paper. To investigate the impact of packet losses on the stability of NCSs, we consider two scenarios. The first is an architecture employing PETMs in the presence of packet losses, whereas the second jointly designs the PETMs and dynamic quantizers for both the sensor-to-controller and controller-to-actuator channels under packet losses, thereby characterizing the effects of quantized signal transmission.

2.1.1. Dynamic PETMs under Packet Losses

As depicted in **Figure 1(a)**, the plant and controller communicate with each other through two decoupled networks, which are denoted as N_1 and N_2. Each of these networks is equipped with an independent dynamic PETM.

For each network N_i with $i\in\{1,2\}$, the signal $v_i\in\mathbb{R}^{n_{v_i}}$ is sampled only at a sequence of discrete sampling instants defined by $t_j^i=jh_i$. Here, $j\in\mathbb{N}$ denotes an arbitrary positive integer, and $h_i>0$ is a positive scalar that represents the sampling period of network N_i. The trigger PETM*i* in network N_i checks the event-triggering condition at these sampling instants. Once the event-triggering condition is satisfied, the trigger PETM*i* is activated, and the data packet containing the latest sampled data is transmitted to the recipient. Let $s_k^i\ (k\in\mathbb{T}_i)$ represent the *k*th triggered instant of the trigger PETM*i*, where $\mathbb{T}_i=\{0,1,2,\cdots\}\subseteq\mathbb{N}$ denotes the index set of all triggered instants. However, due to the inherent unreliability of communication networks, data packet dropouts may occur during transmission. The triggered instant corresponding to the data packet received and adopted by the recipient is called successful, and the r th successful triggered instant is denoted as z_r^i, $r\in\mathbb{S}_i:=\{0,1,2,\cdots\}$. Obviously, the set $\{z_r^i\mid r\in\mathbb{S}_i\}\subset\{s_k^i\mid k\in\mathbb{T}_i\}\subset\{t_j^i\mid j\in\mathbb{N}\}$. In PETC, the sampling period $h_i>0$ is provided to avoid Zeno behaviors. Consequently, both the set $\{t_j^i\mid j\in\mathbb{N}\}$ and $\{s_k^i\mid k\in\mathbb{T}_i\}$ are at most countable and have no finite accumulation point. For convenience, if the set $\mathbb{S}_i$ is finite, *i.e.*, $\mathbb{S}_i=\{0,1,\cdots,r_i^*\}$ for $r_i^*\in\mathbb{N}_{>0}$, we define $z_{r_i^*+1}^i=\infty$.

If the packet at s_k^i is lost, the signal $\hat{v}_i$ available at the receiver is not updated. Between two consecutive successful triggered instants, $\hat{v}_i$ is kept constant with a zero-order-hold (ZOH) device, *i.e.*,

$$\hat{v}_i(t)=v_i(z_r^i),\forall t\in(z_r^i,z_{r+1}^i],r\in\mathbb{S}_i,i\in\{1,2\}.$$

Denote $\delta_r^i\in\Delta_i:=\{0,1,\cdots,\delta_{\max}^i\}$ as the number of successive packet losses in the corresponding network within the time interval (z_r^i,z_{r+1}^i), for $i\in\{1,2\}$. In other words, there are δ_r^i triggered instants in network N_i within the time interval (z_r^i,z_{r+1}^i) at which the transmitted data packets are lost. More precisely, we make the following standard assumption, as commonly adopted in the literature [9].

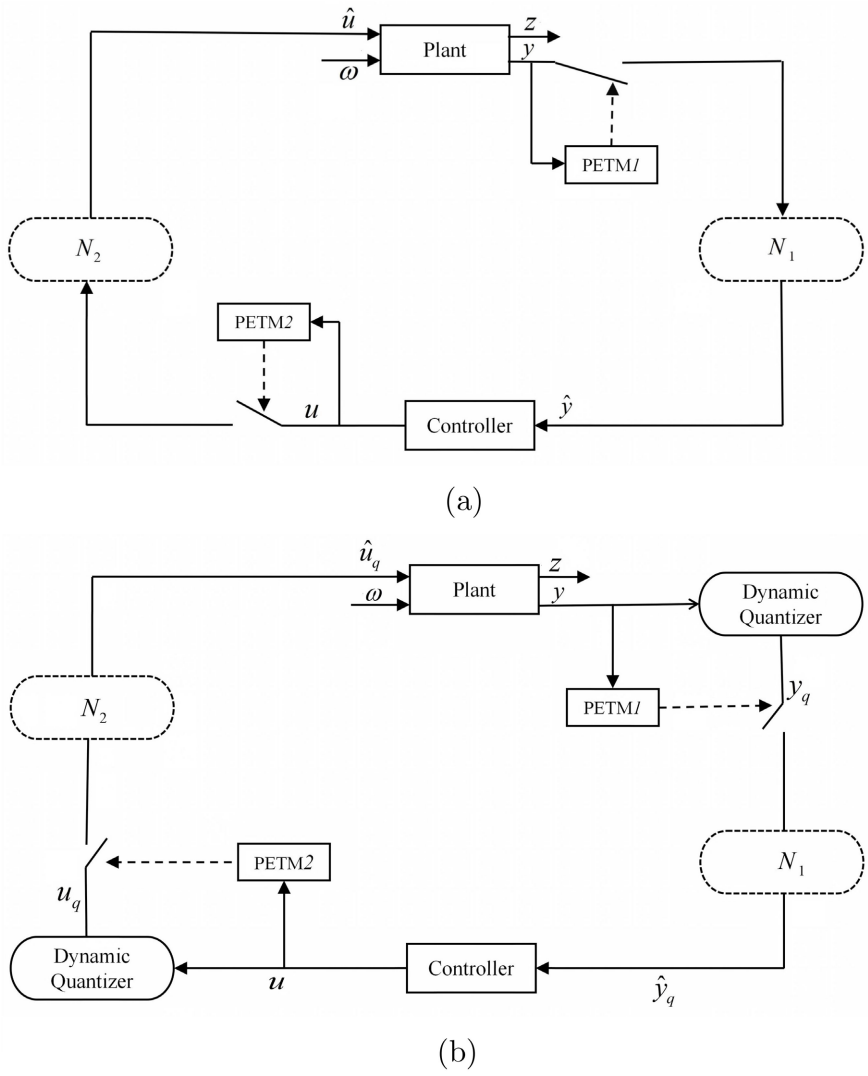

Figure 1. Network architectures considered in this paper. (a) Baseline NCS architecture with dynamic PETMs. (b) Proposed NCS architecture with dynamic PETMs and dynamic quantizers.

Assumption 1. [9] *There exist nonnegative integers* $\delta_{\max}^i \left(i \in \{1,2\}\right)$ *satisfying* $0 \le \delta_r^i \le \delta_{\max}^i \left(r \in \mathbb{S}_i, i \in \{1,2\}\right)$. *Here,* $\delta_{\max}^i$ *represents the maximally allowable numbers of consecutive packet losses in network* N_i.

2.1.2. Dynamic PETMs and Dynamic Quantizers under Packet Losses

As shown in **Figure 1(b)**, the plant and the controller still communicate through two decoupled networks N_1 and N_2. Each network is equipped with an independent dynamic PETM, and a dynamic quantizer is additionally introduced in each communication channel to quantize signals prior to transmission.

For $i \in \{1,2\}$, let $v_{q,i}$ denote the quantized value of v_i and $\hat{v}_{q,i}$ denote the networked version of $v_{q,i}$. For notational simplicity, we further define $v_q = \left(v_{q,1}, v_{q,2}\right)$ and $\hat{v}_q = \left(\hat{v}_{q,1}, \hat{v}_{q,2}\right)$, where $v_{q,1} = y_q$, $v_{q,2} = u_q$, $\hat{v}_{q,1} = \hat{y}_q$ and $\hat{v}_{q,2} = \hat{u}_q$. For network N_i, the signal v_i is sampled only at the sampling in-

stants t_j^i. At each sampling instant, the trigger PETM*i* checks the corresponding triggering condition. When the triggering condition is satisfied at a triggered instant $s_k^i\left(k\in\mathbb{T}_i\right)$, the sampled signal is immediately quantized by the dynamic quantizer. The zoom variable of the dynamic quantizer is encoded and transmitted to the recipient together with the quantized data. The recipient then decodes the received data packet and processes the decoded data. In this scenario, packet dropouts are also considered, with the maximum allowable number of packet dropouts specified in Assumption 1. Between two consecutive successful triggered instants, $\hat{v}_{q,i}$ is also held constant by a ZOH device, *i.e.*,

$$\hat{v}_{q,i}\left(t\right)=v_{q,i}\left(z_r^i\right),\forall t\in\left(z_r^i,z_{r+1}^i\right],r\in\mathbb{S}_i,i\in\{1,2\}.$$

A quantizer in network N_i is essentially a piecewise constant function $q_i:\mathbb{R}^{n_{v_i}}\mapsto\mathbb{Q}_i\subset\mathbb{R}^{n_{v_i}}$, where $\mathbb{Q}_i$ is a finite subset of $\mathbb{R}^{n_{v_i}}$ with finite cardinality $\mathrm{card}\left(\mathbb{Q}_i\right)$. The quantizer q_i generates a partition of $\mathrm{card}\left(\mathbb{Q}_i\right)$ quantization regions in $\mathbb{R}^{n_{v_i}}$, which is described by $\left\{o\in\mathbb{R}^{n_{v_i}}\mid q_i\left(o\right)=w,w\in\mathbb{Q}_i\right\}$. Without loss of generality, we assume that $\mathbb{Q}_i$ is ordered increasingly as a finite list. We adopt the standard quantizer assumption proposed in [22].

Assumption 2. [22] *There exist positive constants* M_i *and* $\aleph_i$ *such that*

$$\left|v_i\right|\le M_i\Rightarrow\left|q_i\left(v_i\right)-v_i\right|\le\aleph_i, \tag{4}$$

where M_i *and* $\aleph_i$ *are referred to as the initial quantization range and initial quantization error bound, respectively.*

The inequality (4) shows that if the quantizer does not saturate, then the quantization error always has an upper bound. Accordingly, we employ the following dynamic quantizer to avoid quantizer saturation.

$$q_{i,\mu_i}\left(v_i\right):=\mu_i q_i\left(\frac{v_i}{\mu_i}\right), \tag{5}$$

where $\mu_i\in\mathbb{R}_{\ge\underline{\mu_i}}$ is the zoom variable associated with the dynamic quantizer q_{i,μ_i}, and $\underline{\mu_i}$ is a lower bound for μ_i (see Section 4.1 for details). The function $q_i\left(\cdot\right)$ satisfies Assumption 2 for some scalars $M_i>0$ and $\aleph_i>0$. At each triggered instant, zoom variable μ_i is updated dynamically based on the magnitude of v_i, thereby scaling the quantization range to $M_i\mu_i$ and the corresponding error bound to $\aleph_i\mu_i$. As a result, inequality (4) becomes

$$\left|v_i\right|\le M_i\mu_i\Rightarrow\left|q_{i,\mu_i}\left(v_i\right)-v_i\right|\le\aleph_i\mu_i. \tag{6}$$

Note that the total number of quantization regions remains unchanged under this dynamic scaling. The zoom variable μ_i is updated at each triggered instant according to the following rule:

$$\mu_i^+=\Omega_{i,out}^{z_{i,out}}\Omega_{i,in}^{z_{i,in}}\mu_i, \tag{7}$$

where $\Omega_{i,out}>1$ and $\Omega_{i,in}\in\left(0,1\right)$ are the zoom-out and zoom-in scaling factors, $z_{i,in}\in\mathbb{Z}$ and $z_{i,out}\in\mathbb{Z}$ denote the number of zoom-in and zoom-out operations

performed at the transmission instant. To ensure synchronous operation, the encoder and decoder are initialized with the same μ_i, and share the common parameters $\Omega_{i,in}$, $\Omega_{i,out}$ and the quantization set $\mathbb{Q}_i$ [23]. Since the decoder cannot directly obtain the current value of μ_i, the integer indices $z_{i,in}$ and $z_{i,out}$ are transmitted over the network to update the decoder-side μ_i.

Having described the architectures of both the baseline and the proposed NCSs, we now detail the dynamic PETM adopted in both cases, which is developed under a unified design framework. In our system configuration, two triggers operate asynchronously and independently in two distinct networks, but all these triggering conditions are designed to take the following form

$$s_{k+1}^i = \inf\left\{t > s_k^i \mid t \in \left\{t_j^i \mid j \in \mathbb{N}\right\} \wedge \min_{t_i \in \Delta_i} \xi_{i,t_i+1} \le 0\right\}, \text{ for } i \in \{1,2\}, \tag{8}$$

where $k \in \mathbb{N}$, the triggering functions $\xi_{i,t_i+1} \in \mathbb{R}$ are to be defined (refer to (24) or (41)).

Remark 1. *From* (8), *one can easily find that the trigger PETMi here periodically detects the values of the triggering functions* ξ_{i,t_i+1} *instead of continuously detecting the values of the dynamic variables* η_{i,t_i+1}, *which is quite different from the triggers in* [9] *in CETC. PETM*1 *and PETM*2 *are deployed in the sensor-to-controller* (*S-C*) *channel and the controller-to-actuator* (*C-A*) *channel, respectively. Under this setup, the scheduled transmission signal vector can be uniformly expressed as* $v = (y,u)$. *It is worth noting that the triggering framework developed in this paper is also applicable to general NCSs with an arbitrary finite number of nodes. For the multi-node case, the scheduled signal vector can be extended to the general form* $v = (v_1, v_2, \cdots, v_n)$, *where* $v_i\ (i = 1,2,\cdots,n)$ *denotes the signal to be transmitted at the i-th network node.*

2.2. Problem Statement

Building on the two network architectures described above, we formulate the control problems considered in this paper. For both scenarios, the objective is to design the communication mechanisms and dynamic output feedback controller such that the resulting closed-loop system is $\mathcal{L}_2$-stable under no-ACK packet losses.

For the baseline NCS equipped solely with dynamic PETMs, the control problem is to co-design the dynamic PETMs in (8) and the dynamic output feedback controller (2) such that the resulting closed-loop system is $\mathcal{L}_2$-stable under no-ACK packet losses. For the proposed NCS with limited communication bandwidth, the dynamic PETMs in (8) and dynamic quantizers in (5) are jointly designed as a unified dynamic periodic event-triggered quantization mechanism (PETQM), together with the dynamic output feedback controller in (2), such that the resulting closed-loop system is $\mathcal{L}_2$-stable in the presence of both quantization errors and packet dropouts.

To rigorously characterize the stability criterion adopted throughout this work,

we recall the definition of $\mathcal{L}_2$-stability as follows:

Definition 1. [30] ($\mathcal{L}_2$-*stable*) *For a system* $\mathcal{H}$ *with initial state* $x(t_0)$ *and external disturbance* $\omega \in \mathcal{L}_2$, *suppose that there exists a* $\mathcal{K}_\infty$-*class function* α *such that solutions* $\phi_{\mathcal{H}}(t)$ *of the system satisfy*

$$\|z\|_{\mathcal{L}_2} \leq \alpha\left(\left|\phi_{\mathcal{H}}(t_0)\right|\right) + \theta\|\omega\|_{\mathcal{L}_2},$$

where $\|z\|_{\mathcal{L}_2} := \left(\sum_{j=0}^{J-1}\int_{t_j}^{t_{j+1}}|z(t)|^2\,\mathrm{d}t\right)^{\frac{1}{2}}$ *denotes the* $\mathcal{L}_2$-*norm of* z. *Then the system* $\mathcal{H}$ *is* $\mathcal{L}_2$-*stable from* ω *to the performance output* z *with an* $\mathcal{L}_2$-*gain less than or equal to* $\theta \in \mathbb{R}_{\geq 0}$.

3. Co-Design of Dynamic PETM and Output Feedback Controller under No-ACK Packet Losses

This section investigates the co-design of the dynamic PETM and the dynamic output feedback controller for the baseline NCS subject to no-ACK packet losses. First, a closed-loop system model under the dynamic PETM is established by characterizing the effects of event-triggered transmission and packet losses. Then, sufficient conditions for $\mathcal{L}_2$-stability are derived in terms of LMIs, and the stability of the resulting closed-loop system is analyzed accordingly. The obtained conditions are further used to determine the parameters of the triggering functions ξ_{i,t_i+1} and the dynamic output feedback controller in (2).

3.1. Closed-Loop System Modeling under the Dynamic PETM

In this section, we establish the closed-loop system for the plant (1) and controller (2) under the dynamic PETM and no-ACK packet losses. The coupled system dynamics are then reorganized into an augmented state-space form for subsequent stability analysis.

For $t \in \left(t_j^i, t_{j+1}^i\right)$, $i \in \{1,2\}$, the closed-loop dynamics are given by

$$\dot{x} = Ax + Be + E\omega, \tag{9}$$

where $A = \begin{bmatrix} A_p & B_pC_c \\ B_cC_p & A_c \end{bmatrix}, B = \begin{bmatrix} 0 & B_p \\ B_c & 0 \end{bmatrix}, E = \begin{bmatrix} E_p \\ 0 \end{bmatrix}$. By the definition of v, we have $v = C_v x$ and $v_i = C_{v,i}x$, with $C_v = \begin{bmatrix} C_p & 0 \\ 0 & C_c \end{bmatrix}$, $C_{v,1} = \begin{bmatrix} C_p & 0 \end{bmatrix}$ and $C_{v,2} = \begin{bmatrix} 0 & C_c \end{bmatrix}$. Consequently,

$$\dot{v}_i = A_{v,i}x + B_{v,i}e + E_{v,i}\omega, \tag{10}$$

where $A_{v,i} = C_{v,i}A$, $B_{v,i} = C_{v,i}B$, $E_{v,i} = C_{v,i}E$. Accordingly, for $t \in \mathbb{R}_{>0}$ and $t \notin \left\{t_j^i \mid j \in \mathbb{N}, i \in \{1,2\}\right\}$, the dynamics of e_i are given by

$$\dot{e}_i = A_{e,i}x + B_{e,i}e + E_{e,i}\omega. \tag{11}$$

Here, $A_{e,i} = -C_{v,i}A$, $B_{e,i} = -C_{v,i}B$, $E_{e,i} = -C_{v,i}E$.

Inspired by [9], we introduce auxiliary variables $\delta_i \in \Delta_i$, $\tau_i \in \mathbb{R}_{\geq 0}$ and two

registers Θ_i for $i \in \{1,2\}$. The auxiliary variable δ_i is used to record the number of successive packet losses of network N_i since its last successful triggered instant. This means that for $t \in \left(z_r^i, z_{r+1}^i\right]$, $\left(r \in \mathbb{S}_i\right)$, the trigger PETM$i$ is triggered $\delta_i(t)$ times within the time interval $\left[z_r^i, t\right)$. The internal clock variables $\tau_i \in \mathbb{R}_{\geq 0}$ measure the elapsed time of network N_i since its last triggered instant, *i.e.*, $\tau_i(t) := t - s_k^i$ for $t \in \left[s_k^i, s_{k+1}^i\right)$. Each network is equipped with a register $\Theta_i := \left(\Theta_{i,1}, \Theta_{i,2}, \cdots, \Theta_{i,\delta_{\max}^i+1}\right)$, which stores the sampled signals corresponding to the most recent $\delta_{\max}^i + 1$ triggered instants. For simplicity, the time argument t is omitted from all variables where appropriate, including $\delta_i(t)$ and $\tau_i(t)$, which are abbreviated to δ_i and τ_i. To design the dynamic PETM to compensate for the effects of consecutive packet losses in no-ACK networks, we introduce a set of dynamic variables $\eta_i = \left(\eta_{i,1}, \eta_{i,2}, \cdots, \eta_{i,\delta_{\max}^i+1}\right) \in \mathbb{R}_{\geq 0}^{\delta_{\max}^i+1}$, where $\eta_{i,\delta_i+1} \in \mathbb{R}_{\geq 0}$ denotes the dynamic variable associated with the current number of consecutive packet losses δ_i, for $i \in \{1,2\}$. These dynamic variables serve as the basis for constructing the triggering functions.

Denote the augmented state by $q := \left(x, e_i, \delta_i, \tau_i, \eta_i, \Theta_i\right) \in \mathbb{R}^{n_x} \times \mathbb{R}^{n_{v_i}} \times \Delta_i \times \mathbb{R}_{\geq 0} \times \mathbb{R}_{\geq 0}^{\delta_{\max}^i+1} \times \mathbb{R}^{\left(\delta_{\max}^i+1\right)n_{v_i}}$, for $i \in \{1,2\}$. Then, the closed-loop system resulting from (1) - (2) is given by

$$\frac{\mathrm{d}}{\mathrm{d}t}\begin{bmatrix} x(t) \\ e_i(t) \\ \delta_i(t) \\ \tau_i(t) \\ \eta_i(t) \\ \Theta_i \end{bmatrix} = \begin{bmatrix} Ax + Be + E\omega \\ A_{e,i}x + B_{e,i}e + E_{e,i}\omega \\ 0 \\ 1 \\ \left(\Upsilon_{i,1}, \cdots, \Upsilon_{i,\delta_{\max}^i+1}\right) \\ \mathbf{0} \end{bmatrix}, \quad t \in \mathbb{R}_{\geq 0}, t \notin \left\{t_j^i \mid j \in \mathbb{N}, i \in \{1,2\}\right\} \tag{12}$$

$$\begin{bmatrix} x\left(t^+\right) \\ e_i\left(t^+\right) \\ \delta_i\left(t^+\right) \\ \tau_i\left(t^+\right) \\ \eta_i\left(t^+\right) \\ \Theta_i\left(t^+\right) \end{bmatrix} = \begin{bmatrix} x \\ e_i \\ \delta_i \\ 0 \\ \left(\xi_{i,1}, \xi_{i,2}, \cdots, \xi_{i,\delta_{\max}^i+1}\right) \\ \Theta_i \end{bmatrix}, \quad \begin{array}{l} t \in \left\{t_j^i \mid j \in \mathbb{N}, i \in \{1,2\}\right\} \setminus \\ \left\{s_k^i \mid k \in \mathbb{T}_i, i \in \{1,2\}\right\}, \end{array} \tag{13}$$

$$\begin{bmatrix} x\left(t^+\right) \\ e_i\left(t^+\right) \\ \delta_i\left(t^+\right) \\ \tau_i\left(t^+\right) \\ \eta_i\left(t^+\right) \\ \Theta_i\left(t^+\right) \end{bmatrix} = \begin{bmatrix} x \\ e_i \\ \delta_i + 1 \\ 0 \\ \left(\eta_{i,0}, \eta_{i,1}, \cdots, \eta_{i,\delta_{\max}^i}\right) \\ \left(v_i, \Theta_{i,1} \cdots, \Theta_{i,\delta_{\max}^i}\right) \end{bmatrix}, \quad \begin{array}{l} t \in \left\{s_k^i \mid k \in \mathbb{T}_i, i \in \{1,2\}\right\} \setminus \\ \left\{z_r^i \mid r \in \mathbb{S}_i, i \in \{1,2\}\right\}, \end{array} \tag{14}$$

$$\begin{bmatrix} x(t^+) \\ e_i(t^+) \\ \delta_i(t^+) \\ \tau_i(t^+) \\ \eta_i(t^+) \\ \Theta_i(t^+) \end{bmatrix} = \begin{bmatrix} x \\ 0 \\ 0 \\ 0 \\ (\eta_{i,0}, \eta_{i,1}, \cdots, \eta_{i,\delta^i_{\max}}) \\ (v_i, \Theta_{i,1}, \cdots, \Theta_{i,\delta^i_{\max}}) \end{bmatrix}, \ \{z^i_r \mid r \in \mathbb{S}_i, i \in \{1,2\}\} \tag{15}$$

where the functions Υ_{i,δ_i+1}, $\eta_{i,0}$ and ξ_{i,δ_i+1} are to be designed, with ξ_{i,δ_i+1} defining the triggering functions in (8) for $\delta_i \in \Delta_i$.

3.2. $\mathcal{L}_2$ -Stability Analysis

Based on the augmented state model established in the previous section, the $\mathcal{L}_2$ -stability of the closed-loop system is analyzed, and sufficient conditions are derived in terms of feasible linear matrix inequalities (LMIs). Based on these conditions, the parameters of the dynamic PETM and the dynamic output feedback controller (2) are co-designed.

Lemma 1. *Given scalars* $\alpha_b \in \mathbb{R}_{>0}$, *if there exist* $\beta_i \in \mathbb{R}_{>0}$, $\gamma_i \in \mathbb{R}_{>0}$, $\alpha_m \geq 0$ *for all* $m \in \{1,2,3\}$, *symmetric positive definite matrices* H_b, X, Y, *and matrices* $\hat{A}_c$, $\hat{B}_c$, $\hat{C}_c$ *satisfying* (16) *and* (17), *then the closed-loop system* (1) - (2) *is* $\mathcal{L}_2$ *-stable and has an* $\mathcal{L}_2$ *-gain from* ω *to* z *less than or equal to* $\theta = \sqrt{\alpha_1 \alpha_2}$.

$$\Omega = \begin{bmatrix} I & * \\ \Omega_1 & 2\alpha_b \Omega_2 - H_b \end{bmatrix} \geq 0, \tag{16}$$

$$\Xi = \begin{bmatrix} \Xi_1^{\mathrm{T}} + \Xi_1 & * & * & * & * & * & * \\ \Xi_2 & -\Gamma & * & * & * & * & * \\ \Xi_3 & 0 & -\alpha_1 I_{n_\omega} & * & * & * & * \\ \Xi_1 & \Xi_2^{\mathrm{T}} & \Xi_3^{\mathrm{T}} & -\frac{1}{\alpha_b^2} H_b & * & * & * \\ \Xi_4 & 0 & 0 & 0 & -\alpha_2 I_{n_z} & * & * \\ \Xi_5 & 0 & 0 & 0 & 0 & -\Phi(\beta) & * \\ \Xi_6 & 0 & 0 & 0 & 0 & 0 & -\alpha_3 I_{n_x} \end{bmatrix} \leq 0, \tag{17}$$

where

$$\Omega_1 = \begin{bmatrix} -C_p^{\mathrm{T}} & 0 \\ -X^{\mathrm{T}} C_p^{\mathrm{T}} & -\hat{C}_c^{\mathrm{T}} \end{bmatrix},$$

$$\Omega_2 = \begin{bmatrix} Y & * \\ I & X^{\mathrm{T}} \end{bmatrix},$$

$$\Xi_1 = \begin{bmatrix} YA_p + \hat{B}_c C_p & \hat{A}_c \\ A_p & A_p X + B_p \hat{C}_c \end{bmatrix},$$

$$\Xi_2 = \begin{bmatrix} \hat{B}_c^{\mathrm{T}} & 0 \\ B_p^{\mathrm{T}} Y & B_p^{\mathrm{T}} \end{bmatrix},$$

$$\Xi_3 = \begin{bmatrix} E_p^{\mathrm{T}} Y & E_p^{\mathrm{T}} \end{bmatrix},$$

$$\Xi_4 = \begin{bmatrix} C_{zp} & C_{zp} X \end{bmatrix},$$

$$\Xi_5 = \begin{bmatrix} C_p & C_p X \\ 0 & \hat{C}_c \end{bmatrix},$$

$$\Xi_6 = \begin{bmatrix} I & X \\ 0 & M^{\mathrm{T}} \end{bmatrix},$$

$$\Gamma = \begin{bmatrix} \gamma_1^2 I_{n_{v1}} & 0 \\ 0 & \gamma_2^2 I_{n_{v2}} \end{bmatrix}$$

$$\hat{A}_c = YA_pX + \hat{B}_c C_p X + YB_p \hat{C}_c + NA_c M^{\mathrm{T}},$$

$$\hat{B}_c = NB_c, \hat{C}_c = C_c M^{\mathrm{T}}$$

$$\Phi(\beta) = \begin{bmatrix} \beta_1 I_{n_{v1}} & 0 \\ 0 & \beta_2 I_{n_{v2}} \end{bmatrix}.$$

Proof. Define

$$Z_1 = \begin{bmatrix} Y & I \\ N^{\mathrm{T}} & 0 \end{bmatrix}, \ Z_2 = \begin{bmatrix} I & X \\ 0 & M^{\mathrm{T}} \end{bmatrix},$$

and let $P = Z_1 Z_2^{-1} = Z_2^{-\mathrm{T}} Z_1^{\mathrm{T}}$. Since $P = P^{\mathrm{T}} > 0$, it follows that $XY + MN^{\mathrm{T}} = I$. Consequently,

$$\Omega_1 = -Z_2^{\mathrm{T}} C_v^{\mathrm{T}}, \ \Omega_2 = Z_2^{\mathrm{T}} Z_1, \ \Xi_1 = Z_1^{\mathrm{T}} A Z_2,$$

$$\Xi_2 = B^{\mathrm{T}} Z_1, \ \Xi_3 = E^{\mathrm{T}} Z_1, \ \Xi_4 = C_z Z_2,$$

$$\Xi_5 = C_v Z_2, \ \Xi_6 = Z_2.$$

Pre-multiplying and post-multiplying (17) by $\mathrm{diag}\left\{Z_2^{-\mathrm{T}}, I, I, Z_2^{-\mathrm{T}}, I, II\right\}$ and its transpose, respectively, yields

$$\begin{bmatrix} PA + A^{\mathrm{T}} P & * & * & * & * & * & * \\ B^{\mathrm{T}} P & -\Gamma & * & * & * & * & * \\ E^{\mathrm{T}} P & 0 & -\alpha_1 I_{n_\omega} & * & * & * & * \\ PA & PB & PE & -\dfrac{1}{\alpha_b^2} \hat{H}_b & * & * & * \\ C_z & 0 & 0 & 0 & -\alpha_2 I_{n_x} & * & * \\ C_v & 0 & 0 & 0 & 0 & -\Phi(\beta) & * \\ I & 0 & 0 & 0 & 0 & 0 & -\alpha_3 I_{n_x} \end{bmatrix} \leq 0,$$

where $\hat{H}_b = Z_2^{-\mathrm{T}} H_b Z_2^{-1}$. Applying the Schur complement to the above inequality yields that

$$\begin{bmatrix} PA+A^{\mathrm{T}}P+\dfrac{1}{\alpha_2}C_z^{\mathrm{T}}C_z+C_v^{\mathrm{T}}\Phi(\beta)^{-1}C_v+\dfrac{1}{\alpha_3}I_{n_x} & * & * \\ B^{\mathrm{T}}P & -\Gamma & * \\ E^{\mathrm{T}}P & 0 & -\alpha_1 I_{n_\omega} \end{bmatrix} + \begin{bmatrix} A^{\mathrm{T}}P \\ B^{\mathrm{T}}P \\ E^{\mathrm{T}}P \end{bmatrix} \alpha_b^2 \hat{H}_b^{-1} \begin{bmatrix} PA & PB & PE \end{bmatrix} \le 0. \tag{18}$$

It follows from (16) that $2\alpha_b Z_2^{\mathrm{T}} Z_1 - H_b \ge Z_2^{\mathrm{T}} C_v^{\mathrm{T}} C_v Z_2$. Moreover, by Young's inequality, $C_v^{\mathrm{T}} C_v \le 2\alpha_b P - \hat{H}_b \le \alpha_b^2 P \hat{H}_b^{-1} P$, and hence

$$\begin{bmatrix} PA+A^{\mathrm{T}}P+\dfrac{1}{\alpha_2}C_z^{\mathrm{T}}C_z+C_v^{\mathrm{T}}\Phi(\beta)^{-1}C_v+\dfrac{1}{\alpha_3}I_{n_x} & * & * \\ B^{\mathrm{T}}P & -\Gamma & * \\ E^{\mathrm{T}}P & 0 & -\alpha_1 I_{n_\omega} \end{bmatrix} + \begin{bmatrix} A^{\mathrm{T}} \\ B^{\mathrm{T}} \\ E^{\mathrm{T}} \end{bmatrix} C_v^{\mathrm{T}} C_v \begin{bmatrix} A & B & E \end{bmatrix} \le 0,$$

from which it follows that

$$\begin{bmatrix} \Sigma_1 & * & * \\ B^{\mathrm{T}}P+B_e^{\mathrm{T}}A_e & B_e^{\mathrm{T}}B_e-\Gamma & * \\ E^{\mathrm{T}}P+E_e^{\mathrm{T}}A_e & E_e^{\mathrm{T}}B_e & E_e^{\mathrm{T}}E_e-\alpha_1 I_{n_\omega} \end{bmatrix} \le 0, \tag{19}$$

where $\Sigma_1 := PA+A^{\mathrm{T}}P+\dfrac{1}{\alpha_2}C_z^{\mathrm{T}}C_z+C_v^{\mathrm{T}}\Phi(\beta)^{-1}C_v+\dfrac{1}{\alpha_3}I_{n_x}+A_e^{\mathrm{T}}A_e$,

$A_e = C_v A = \begin{bmatrix} -A_{e,1} \\ -A_{e,2} \end{bmatrix}$, $B_e = C_v B = \begin{bmatrix} -B_{e,1} \\ -B_{e,2} \end{bmatrix}$, and $E_e = C_v E = \begin{bmatrix} -E_{e,1} \\ -E_{e,2} \end{bmatrix}$.

Consider the quadratic function $V(x) = x^{\mathrm{T}}Px$. Its derivative along the trajectories of (1) - (2) is given by $\dot{V}(x) = x^{\mathrm{T}}\left(A^{\mathrm{T}}P+PA\right)x + 2e^{\mathrm{T}}B^{\mathrm{T}}Px + 2\omega^{\mathrm{T}}E^{\mathrm{T}}Px$. From (19), the derivative of $V(x)$ satisfies

$$\begin{aligned} &\left\langle \nabla V(x), Ax+Be+E\omega \right\rangle \\ &\le -\sigma|x|^2 + \sum_{i=1}^{2}\left(-\varrho_i|v_i|^2+\gamma_i^2|e_i|^2-\left(A_{e,i}x+B_{e,i}e+E_{e,i}\omega\right)^{\mathrm{T}}\left(A_{e,i}x+B_{e,i}e+E_{e,i}\omega\right)\right) \\ &\quad +\mu\left(\theta^2|\omega|^2-|z|^2\right), \end{aligned} \tag{20}$$

where $\sigma = \dfrac{1}{\alpha_3}$, $\varrho_i = \dfrac{1}{\beta_i}$, and $\mu = \dfrac{1}{\alpha_2}$, for all $x \in \mathbb{R}^{n_x}$, $e \in \mathbb{R}^{n_v}$ and $\omega \in \mathbb{R}^{n_\omega}$. In the absence of network-induced errors, *i.e.*, $e = 0$, the above dissipation inequality establishes the $\mathcal{L}_2$-stability of the nominal closed-loop system with an $\mathcal{L}_2$-gain no greater than θ.

□

The above dissipation inequality provides a basis for constructing the Lyapunov function of the overall networked closed-loop system. We next present the co-de-

sign of the dynamic PETMs and the dynamic output feedback controller (2), followed by the stability analysis of the closed-loop system (12) - (15).

Theorem 1. *Suppose that the conditions in* (16) - (17) *of Lemma 1 hold. If there exist positive constants* $\mathcal{T}_{\mathrm{MATI}}^{i}$ *satisfying*

$$\left(\delta_{\max}^{i}+1\right)h_i<\mathcal{T}_{\mathrm{MATI}}^{i}, \tag{21}$$

then, under the following choices of the dynamic PETMS and the dynamic output feedback controller, the closed-loop system (12) - (15) *is* $\mathcal{L}_2$ *-stable with an* $\mathcal{L}_2$ *-gain less than or equal to* θ. *Choose*

$$\Upsilon_{i,\delta_i+1}=\varrho_i\left|v_i\right|^2,\ \delta_i\in\Delta_i. \tag{22}$$

At each triggering instant $s_k^i, k\in\mathbb{T}_i$, *the dynamic variables* η_{i,δ_i+1} *are updated according to* (14) *or* (15), *together with*

$$\eta_{i,1}^{+}=\eta_{i,0}:=\min_{k\in\Delta_i}\left\{\gamma_i\phi_i\left(\left(k+1\right)h_i\right)\left|\Theta_{i,k+1}-v_i\right|^2+\eta_{i,k+1}\right\}. \tag{23}$$

The triggering functions ξ_{i,δ_i+1} *are given at the sampling instants* $\left\{t_j^i\mid j\in\mathbb{N},i\in\{1,2\}\right\}$ *by*

$$\xi_{i,\delta_i+1}=\gamma_i\left(\phi_i\left(\left(\delta_i+1\right)h_i\right)-\phi_i\left(\delta_i h_i\right)\right)\left|\Theta_{i,\delta_i+1}-v_i\right|^2+\eta_{i,\delta_i+1}. \tag{24}$$

The matrices A_c, B_c *and* C_c *of the dynamic output feedback controller are then obtained from*

$$\begin{bmatrix}A_c & B_c\\ C_c & 0\end{bmatrix}=\begin{bmatrix}N & YB_p\\ 0 & I\end{bmatrix}^{-1}\begin{bmatrix}\hat{A}_c-YA_pX & \hat{B}_c\\ \hat{C}_c & 0\end{bmatrix}\begin{bmatrix}M^{\mathrm{T}} & 0\\ C_pX & I\end{bmatrix}^{-1}. \tag{25}$$

Proof. For $t\geq 0$, consider the following piecewise continuous Lyapunov function:

$$U\left(t\right)=V\left(x\right)+\sum_{i=1}^{2}\left(\gamma_i\phi_i\left(\delta_i h_i+\tau_i\right)\left|e_i\right|^2+\eta_{i,\delta_i+1}\right), \tag{26}$$

where $V\left(x\right)=x^{\mathrm{T}}Px$ with $P>0$, $\gamma_i>0$ are given in Lemma 1 and the functions $\phi_i:\mathbb{R}_{\geq 0}\to\mathbb{R}_{\geq 0}$ satisfy

$$\dot{\phi}_i\left(s\right)=-\gamma_i\left(\phi_i^2\left(s\right)+1\right). \tag{27}$$

For each $i\in\{1,2\}$, choose $\lambda_i\in(0,1)$ and $\phi_i\left(0\right)=\lambda_i^{-1}$. Solving (27) gives $\phi_i\left(s\right)=\tan\left(\arctan\left(\lambda_i^{-1}\right)-\gamma_i s\right)$. Define $\mathcal{T}_{\mathrm{MATI}}^{i}=\left[\arctan\left(\lambda_i^{-1}\right)-\arctan\left(\lambda_i\right)\right]\Big/\gamma_i$. Then, $\phi_i\left(\mathcal{T}_{\mathrm{MATI}}^{i}\right)=\lambda_i$, and $\phi_i\left(s\right)\in\left[\lambda_i,\lambda_i^{-1}\right]$ for $0\leq s\leq\mathcal{T}_{\mathrm{MATI}}^{i}$. Hence, a sampling period is any h_i satisfying $0<h_i<\mathcal{T}_{\mathrm{MATI}}^{i}\Big/\left(\delta_{\max}^{i}+1\right)$.

The stability analysis follows the general Lyapunov-based methodology developed in [9] [16] [30] for dynamic ETC. Specifically, to establish the $\mathcal{L}_2$ -stability of the closed-loop system (12) - (15) with the proposed dynamic PETM and dynamic output feedback controller (2), it is sufficient to show that the constructed Lyapunov function U satisfies the following properties:

a) For all $t\in\mathbb{R}_{\geq 0}$, there exist class-$\mathcal{K}_\infty$ functions $\underline{a}_U$ and $\overline{a}_U$ such that

$$\underline{a}_U\left(|q|\right) \le U\left(t\right) \le \overline{a}_U\left(|q|\right); \tag{28}$$

b) For all $t \in \left\{t_j^i \mid j \in \mathbb{N}, i \in \{1,2\}\right\}$, it holds that

$$U\left(t^+\right) - U\left(t\right) \le 0; \tag{29}$$

c) For all $t \ge 0$ within inter-sampling intervals, *i.e.*, $t \notin \left\{t_j^i \mid j \in \mathbb{N}, i \in \{1,2\}\right\}$, it holds that

$$\dot{U}\left(t\right) \le -\sigma|x|^2 + \mu\left(\theta^2|\omega|^2 - |z|^2\right). \tag{30}$$

We first verify property **a)**. By construction of the dynamic variables $\eta_{i,\delta_i+1} \ge 0$ for all $i \in \{1,2\}$. Thus, $U\left(t\right)$ satisfies $\lambda_{\min}\left(P\right)|x|^2 + \sum_{i=1}^2\left(\gamma_i\lambda_i|e_i|^2 + \eta_{i,\delta_i+1}\right) \le U\left(t\right) \le \lambda_{\max}\left(P\right)|x|^2 + \sum_{i=1}^2\left(\gamma_i\lambda_i^{-1}|e_i|^2 + \eta_{i,\delta_i+1}\right)$. Since the lower and upper bounds are positive definite and radially unbounded functions of the augmented state q, they can be bounded by suitable class-$\mathcal{K}_\infty$ functions. Hence, there exist class-$\mathcal{K}_\infty$ functions $\underline{a}_U$ and $\overline{a}_U$ such that (28) holds. This verifies statement **a)**.

Now, we proceed to verify statement **b)**, which states that the Lyapunov function U is non-increasing at jump points. To facilitate the subsequent analysis, define $U_i\left(t\right) = \gamma_i\phi_i\left(\delta_i h_i + \tau_i\right)|e_i|^2 + \eta_{i,\delta_i+1}$.

Consider the sampling instants at which no triggering occurs, *i.e.*, $\left\{t_j^i \mid j \in \mathbb{N}\right\} \setminus \left\{s_k^i \mid k \in \mathbb{T}_i\right\}$. At these instants, the post-jump variables satisfy $\delta_i^+ = \delta_i$, $\tau_i^+ = 0$ (with $\tau_i = h_i$), $e_i^+ = e_i = \Theta_{i,\delta_i+1} - v_i$, and $\eta_{i,\delta_i+1}^+ = \xi_{i,\delta_i+1}$. Consequently,

$$U_i\left(t^+\right) - U_i\left(t\right) = \gamma_i\phi_i\left(\delta_i h_i\right)|e_i|^2 + \xi_{i,\delta_i+1} - \left(\gamma_i\phi_i\left(\delta_i h_i + h_i\right)|e_i|^2 + \eta_{i,\delta_i+1}\right).$$

By the triggering function (24), it follows that $U\left(t^+\right) - U\left(t\right) \le 0$. Moreover, the triggering condition (8) ensures that the updated value of η_{i,δ_i+1} satisfies $\eta_{i,\delta_i+1}^+ = \xi_{i,\delta_i+1} > 0$.

For the triggered instants at which the transmitted packet is lost, *i.e.*, $t \in \left\{s_k^i \mid k \in \mathbb{T}_i\right\} \setminus \left\{z_r^i \mid r \in \mathbb{S}_i\right\}$, we have $\delta_i^+ = \delta_i + 1$, $\tau_i^+ = 0$ (with $\tau_i = h_i$) and $e_i^+ = e_i$. Substituting these relations into $U_i\left(t\right)$ gives

$$U_i\left(t^+\right) = \gamma_i\phi_i\left(\left(\delta_i + 1\right)h_i\right)|e_i|^2 + \eta_{i,\delta_i+2}^+,$$

$$U_i\left(t\right) = \gamma_i\phi_i\left(\delta_i h_i + h_i\right)|e_i|^2 + \eta_{i,\delta_i+1}.$$

By (14), $\eta_{i,\delta_i+2}^+ = \eta_{i,\delta_i+1}$, and hence $U\left(t^+\right) - U\left(t\right) \le 0$ still holds.

For the successful triggered instants $t \in \left\{z_r^i \mid r \in \mathbb{S}_i, i \in \{1,2\}\right\}$, we have $\delta_i^+ = 0$, $\tau_i^+ = 0$ (with $\tau_i = h_i$), and $e_i^+ = 0$. Then,

$$U_i\left(t^+\right) - U_i\left(t\right) = \gamma_i\phi_i\left(0\right)|0|^2 + \eta_{i,1}^+ - \left(\gamma_i\phi_i\left(\delta_i h_i + h_i\right)|e_i|^2 + \eta_{i,\delta_i+1}\right).$$

By the definition of $\eta_{i,1}^+$ in (23) and its upper bound

$$\eta_{i,0} \le \overline{\eta}_i \triangleq \gamma_i\phi_i\left(\left(\delta_i + 1\right)h_i\right)|e_i|^2 + \eta_{i,\delta_i+1}, \tag{31}$$

we have $0 \le \eta_{i,1}^+ \le \overline{\eta}_i$. This follows from the fact that, for any t with $\delta_i \in \Delta_i$, the network-induced error satisfies $e_i = \Theta_{i,\delta_i+1} - v_i$. Accordingly, $U\left(t^+\right) - U\left(t\right) \le 0$.

Thus, statement **b)** is verified.

It remains to verify statement **c)**. Consider the flow dynamics for $t \in \mathbb{R}_{\geq 0} \setminus \left\{ t_j^i \mid j \in \mathbb{N}, i \in \{1,2\} \right\}$. Taking the time derivative of $U(t)$ along the system trajectories yields

$$\dot{U}(t) = \left\langle \nabla V(x), Ax + Be + E\omega \right\rangle + \sum_{i=1}^{2} \left(\gamma_i \dot{\phi}_i (\delta_i h_i + \tau_i) |e_i|^2 + 2\gamma_i \phi_i (\delta_i h_i + \tau_i) |e_i| \frac{\mathrm{d}}{\mathrm{d}t} |e_i| + \Upsilon_{i,\delta_i+1} \right).$$

By Lemma 1, we have

$$\begin{aligned} \dot{U}(t) \leq & -\sigma |x|^2 + \sum_{i=1}^{2} \Big(-\varrho_i |v_i|^2 + \gamma_i^2 |e_i|^2 - \left(A_{e,i} x + B_{e,i} e + E_{e,i} \omega \right)^{\mathrm{T}} \left(A_{e,i} x \right. \\ & \left. + B_{e,i} e + E_{e,i} \omega \right) + \gamma_i \left(-\gamma_i \left(\phi_i^2 (\delta_i h_i + \tau_i) + 1 \right) \right) |e_i|^2 \\ & + 2\gamma_i \phi_i (\delta_i h_i + \tau_i) |e_i| \left| A_{e,i} x + B_{e,i} e + E_{e,i} \omega \right| + \Upsilon_{i,\delta_i+1} \Big) \\ & + \mu \left(\theta^2 |\omega|^2 - |z|^2 \right). \end{aligned}$$

Applying Young's inequality to the cross term and substituting the resulting bound into the above inequality, we obtain

$$\begin{aligned} & 2\gamma_i \phi_i (\delta_i h_i + \tau_i) |e_i| \times \left| A_{e,i} x + B_{e,i} e + E_{e,i} \omega \right| \\ & \leq \gamma_i^2 \phi_i^2 (\delta_i h_i + \tau_i) |e_i|^2 + \left(A_{e,i} x + B_{e,i} e + E_{e,i} \omega \right)^{\mathrm{T}} \left(A_{e,i} x + B_{e,i} e + E_{e,i} \omega \right) \end{aligned}$$

$$\dot{U}(t) \leq -\sigma |x|^2 + \sum_{i=1}^{2} \left(-\varrho_i |v_i|^2 + \Upsilon_{i,\delta_i+1} \right) + \mu \left(\theta^2 |\omega|^2 - |z|^2 \right).$$

By the definition of Υ_{i,δ_i+1}, we have $\dot{U}(t) \leq -\sigma |x|^2 + \mu \left(\theta^2 |\omega|^2 - |z|^2 \right)$. This establishes statement **c)**.

□

Remark 2. *In the above stability analysis, we employ the fundamental norm-derivative inequality* $\frac{\mathrm{d}}{\mathrm{d}t} |e_i| \leq |\dot{e}_i| = \left| A_{e,i} x + B_{e,i} e + E_{e,i} \omega \right|$. *It is worth noting that this treatment of the error derivative bound differs from Condition* 1 *in* [19] *and Assumption* 1 *in* [31]. *For the linear closed-loop system* (1) - (2) *considered in this paper, one can verify that* $B_{e,1} e = -C_p B_p e_2$ *and* $B_{e,2} e = -C_c B_p e_1$. *This implies that, under the frameworks of* [19] *and* [31], *the Lipschitz constants* L_i *associated with* e_i *can be taken to be zero. Consequently, the differential equation for* ϕ_i *preserves the form given in* (27), *without the additional term* $-2L_i \phi_i$. *This simplification yields a relatively slower decay rate of* ϕ_i, *which may allow for a larger sampling interval* h_i *under the event-triggered scheme and thus potentially improve communication efficiency.*

Remark 3. *For numerical implementation,* $\alpha_b > 0$ *is fixed beforehand. By introducing* $g_i = \gamma_i^2$, *the decision variables are* $X, Y, H_b, \hat{A}_c, \hat{B}_c, \hat{C}_c$ *and the scalars* $\alpha_1, \alpha_2, \alpha_3, \beta_i, g_i$, *subject to the required positivity conditions. The hatted controller matrices are treated as independent variables, and their defining relations are used only for controller reconstruction after solving. For each fixed* α_b, *condi-*

tions (16) - (17) *are affine in the decision variables and can be solved as a single SDP feasibility problem. A feasible solution gives* $\gamma_i = \sqrt{g_i}$ *and* $\varrho_i = 1/\beta_i$, *and the controller is recovered using* (25). *The gain bound* $\theta = \sqrt{\alpha_1 \alpha_2}$ *is calculated afterwards and is not minimized in this feasibility problem. If different values of* α_b *are considered, an outer search over a prescribed finite set of positive values is performed, with one SDP solved for each value.*

4. Dynamic Periodic Event-Triggered Quantization and Dynamic Output Feedback Control: Co-Design under No-ACK Packet Losses

In this section, we investigate the co-design of the dynamic PETQM and the dynamic output feedback controller for NCSs subject to no-ACK packet losses, as illustrated in Figure 2. First, the parameters of the dynamic quantizers are designed to ensure proper quantization. Then, the closed-loop system model under the dynamic PETQM is established by characterizing the effects of event-triggered quantization and packet losses. Finally, sufficient conditions for $\mathcal{L}_2$-stability are derived in terms of LMIs, based on which the parameters of the dynamic PETQM and the parameters of the dynamic output feedback controller are determined.

4.1. Parameter Design for Dynamic Quantizers

The i-th dynamic quantizer depicted in Figure 2 incorporates a zoom variable μ_i, whose evolution is governed by the update law in (7). The zoom variable is adjusted according to the normalized magnitude of the transmitted signal relative to the current zoom level. Specifically, its update law is given by

$$\mu_i^+ = \begin{cases} \Omega_{i,in}^{z_{i,in}} \mu_i, & |v_i| \le \ell_{i,in} \mu_i \\ \mu_i, & \ell_{i,in} \mu_i < |v_i| < \ell_{i,out} \mu_i \\ \Omega_{i,out}^{z_{i,out}} \mu_i, & |v_i| \ge \ell_{i,out} \mu_i \end{cases} \tag{32}$$

where constants $\ell_{i,in}$, ℓ_i, $\ell_{i,out}$ satisfy

$$0 < \ell_{i,in} \le \frac{1}{\Omega_{i,out}} \ell_i \le \ell_i \le \frac{1}{\Omega_{i,in}} \ell_i \le \ell_{i,out} \le M_i - \aleph_i, \tag{33}$$

the integer codes $z_{i,in}$ and $z_{i,out}$ are defined as

$$z_{i,in} = \left\lceil \max\left\{ -\nu, \frac{\log\left(\max\left\{ \frac{|v_i|}{\ell_i \mu_i}, \frac{\varphi_i}{\mu_i} \right\} \right)}{\log\left(\Omega_{i,in}\right)} \right\} \right\rceil, \tag{34}$$

$$z_{i,out} = \left\lceil \max\left\{ -\nu, \frac{\log\left(\frac{|v_i|}{\ell_i \mu_i} \right)}{\log\left(\Omega_{i,out}\right)} \right\} \right\rceil, \tag{35}$$

where $\nu \in (0,1)$. The auxiliary function $\varphi_i : \mathbb{R}_{\ge 0} \to \mathbb{R}_{\ge 0}$ is introduced to limit the

amount of zoom-in at each triggered instant. Specifically, φ_i provides a time-varying reference level for the zoom variable, preventing μ_i from shrinking excessively fast under consecutive zoom-in operations. By choosing $\dot{\varphi}_i(t) = -c_i\varphi_i(t)$ with $c_i > 0$ and $\varphi_i(0) > 0$, we have $\varphi_i(t) = \varphi_i(0)\mathrm{e}^{-c_i t}$, so that the reference level remains positive while converging to zero, thereby avoiding a nonzero lower bound on the quantization scale.

Since $-1 < -\nu < 0$, we have $\lceil -\nu \rceil = 0$, which guarantees $z_{i,in}, z_{i,out} \in \mathbb{N}$. It follows from (34) and (35) that

$$z_{i,in} > 0 \Rightarrow \max\left\{\frac{|v_i|}{\ell_i\mu_i}, \frac{\varphi_i}{\mu_i}\right\} < 1 \Rightarrow \frac{|v_i|}{\ell_i\mu_i} < 1 \Rightarrow z_{i,out} = 0,$$

$$z_{i,out} > 0 \Rightarrow \frac{|v_i|}{\ell_i\mu_i} > 1 \Rightarrow \max\left\{\frac{|v_i|}{\ell_i\mu_i}, \frac{\varphi_i}{\mu_i}\right\} > 1 \Rightarrow z_{i,in} = 0. \tag{36}$$

This confirms that zoom-in and zoom-out actions are mutually exclusive at each triggered instant and never occur simultaneously. At a triggered instant $s_k^i \left(k \in \mathbb{T}\right)$, the zoom variable μ_i is updated according to (7). If a zoom-in event occurs, then

$$\Omega_{i,in} \max\left\{\frac{|v_i|}{\ell_i\mu_i}, \frac{\varphi_i}{\mu_i}\right\}\mu_i < \mu_i^+ = \Omega_{i,in}^{z_{i,in}}\mu_i \le \max\left\{\frac{|v_i|}{\ell_i\mu_i}, \frac{\varphi_i}{\mu_i}\right\}\mu_i.$$

If a zoom-out event occurs, then

$$\frac{|v_i|}{\ell_i} \le \mu_i^+ = \Omega_{i,out}^{z_{i,out}}\mu_i < \Omega_{i,out}\frac{|v_i|}{\ell_i}.$$

If neither zoom-in nor zoom-out occurs, then

$$\frac{|v_i|}{\ell_{i,out}} < \mu_i^+ < \frac{|v_i|}{\ell_{i,in}}.$$

Combining these three cases with (33) yields the following bound on the update value μ_i^+

$$\frac{|v_i|}{\ell_{i,out}} < \mu_i^+ \le \max\left\{\frac{|v_i|}{\ell_{i,in}}, \varphi_i\right\}. \tag{37}$$

The term $\dfrac{|v_i|}{\ell_{i,out}}$ in the lower bound ensures that the quantization interval covers the current signal amplitude. This dynamic quantization scheme adaptively adjusts the quantization range through discrete zooming steps to accommodate signal variations and avoid quantizer saturation.

Since the decoder has no direct access to the zoom variable μ_i, only the corresponding update codes $z_{i,in}$ and $z_{i,out}$ are transmitted over the communication network. Given that $\Omega_{i,in}$ and $\Omega_{i,out}$ are known a priori at the decoder, the zoom variable μ_i can be reconstructed according to the update law in (7) upon successful packet reception. To maintain encoder-decoder synchronization in no-ACK networks with bounded consecutive packet losses, we adopt the encoder-decoder framework developed in [16]. Each transmitted packet contains the zoom

updates associated with the $\delta_{\max}^{i}+1$ most recent triggering events. As long as the number of consecutive packet losses does not exceed $\delta_{\max}^{i}$, each successfully received packet contains all zoom updates missed since the last successful reception. The decoder can therefore recover the zoom updates missed during consecutive packet losses and resynchronize its zoom variable with that of the encoder upon each successful packet reception, without requiring a reverse acknowledgment channel.

Remark 4. *The dynamic zooming mechanism in this work is rooted in the dynamic quantization framework of* [22], *which employs online adjustments of the quantization scale. The use of the time-varying variable* φ_i *in the dynamic quantizer is inspired by the dynamic quantization idea in* [10]. *However, unlike the approach in* [10], *which relies on ACK signals to implement the proposed CETC, the proposed dynamic PETQM is developed under a no-ACK communication mechanism. In contrast to these existing approaches, the proposed mechanism embeds this dynamic quantization idea into a discrete multi-step zooming scheme and further integrates it with a no-ACK packet loss framework, with the zooming information designed to enable resynchronization after consecutive packet losses.*

4.2. Closed-Loop System Modeling under the Dynamic PETQM

Unlike the baseline NCS in Section 3, the introduction of dynamic quantizers changes the content stored in the register Θ_i. Specifically, Θ_i stores the quantized values $v_{q,i}$ generated at the most recent $\delta_{\max}^{i}+1$ triggered instants, rather than the corresponding raw signal values. Accordingly, the update rule of the register at triggered instants is given by

$$\Theta_i = \left(v_{q,i}, \Theta_{i,2}, \cdots, \Theta_{i,\delta_{\max}^{i}+1}\right),$$

which differs from the register update rule in (14) - (15). Furthermore, the quantization error and the sampling error are defined as $e_{q,i} := v_{q,i} - v_i$, $e_{s,i} := \hat{v}_{q,i} - v_{q,i}$, respectively. Accordingly, the network-induced error can be decomposed as $e_i := e_{s,i} + e_{q,i} = \hat{v}_{q,i} - v_i$. At successful triggered instants, e_i no longer follows the jump rule in (15); instead, its jump rule is revised to $e_i^+ = e_{q,i}$.

For $t \in \mathbb{R}_{\geq 0} \setminus \left\{t_j^i \mid j \in \mathbb{N}, i \in 1,2\right\}$, the augmented state q evolves according to (12). For $t \in \left\{t_j^i \mid j \in \mathbb{N}, i \in 1,2\right\} \setminus \left\{s_k^i \mid k \in \mathbb{T}_i, i \in 1,2\right\}$, it evolves according to (13). To save space, only the jump rule of the augmented state q at triggered instants is detailed herein.

$$\begin{bmatrix} x(t^+) \\ e_i(t^+) \\ \delta_i(t^+) \\ \tau_i(t^+) \\ \eta_i(t^+) \\ \Theta_i(t^+) \end{bmatrix} = \begin{bmatrix} x \\ e_i \\ \delta_i + 1 \\ 0 \\ \left(\zeta_{i,0}, \eta_{i,1}, \cdots, \eta_{i,\delta_{\max}^{i}}\right) \\ \left(v_{q,i}, \Theta_{i,1}, \cdots, \Theta_{i,\delta_{\max}^{i}}\right) \end{bmatrix}, \quad t \in \left\{s_k^i \mid k \in \mathbb{T}_i, i \in \{1,2\}\right\} \setminus \left\{z_r^i \mid r \in \mathbb{S}_i, i \in \{1,2\}\right\}, \tag{38}$$

$$\begin{bmatrix} x(t^+) \\ e_i(t^+) \\ \delta_i(t^+) \\ \tau_i(t^+) \\ \eta_i(t^+) \\ \Theta_i(t^+) \end{bmatrix} = \begin{bmatrix} x \\ e_{q,i} \\ 0 \\ 0 \\ \left(\zeta_{i,0}, \eta_{i,1}, \cdots, \eta_{i,\delta^i_{\max}}\right) \\ \left(v_{q,i}, \Theta_{i,1}, \cdots, \Theta_{i,\delta^i_{\max}}\right) \end{bmatrix}, \ \left\{z^i_r \mid r \in \mathbb{S}_i, i \in \{1,2\}\right\} \tag{39}$$

where $\zeta_{i,0}$ in (38) - (39), Υ_{i,δ_i+1} in (12), and the triggering functions are designed to guarantee the desired well-posed behavior of the closed-loop system composed of the plant (1) and the controller (2) under the proposed dynamic PETQM. For all $\delta_i \in \Delta_i$, the triggering functions ξ_{i,δ_i+1} in (13) are constructed based on the dynamic functions η_{i,δ_i+1}.

4.3. Stability Analysis for the Dynamic PETQM

The following theorem provides sufficient conditions for the $\mathcal{L}_2$-stability of the closed-loop system under the dynamic PETQM.

Theorem 2. *Suppose that the conditions in* (16) - (17) *of Lemma 1 hold and that there exist positive constants* $\mathcal{T}^i_{\mathrm{MATI}}$ *satisfying* (21). *Let the functions* Υ_{i,δ_i+1} *satisfy* $\Upsilon_{i,\delta_i+1} = (\varrho_i - \epsilon_i)|v_i|^2$ *with* $0 < \epsilon_i < \varrho_i$ *for all* $\delta_i \in \Delta_i$. *At each triggering instant* $\left\{s^i_k \mid k \in \mathbb{T}_i, i \in \{1,2\}\right\}$, *the dynamic variables* η_{i,δ_i+1} *are updated according to* (38) *or* (39), *and*

$$\begin{aligned} \eta^+_{i,1} = \zeta_{i,0} := \min_{k \in \Delta_i} \Big\{ \eta_{i,k+1} + \max\left\{\theta_{i,1}|v_i|^2, \varphi_i^2, \gamma_i \phi_i\left((k+1)h_i\right)\left|\Theta_{i,k+1} - v_i\right|^2\right\} \Big\} \\ - \max\left\{\theta_{i,1}|v_i|^2, \varphi_i^2\right\}. \end{aligned} \tag{40}$$

The triggering functions ξ_{i,δ_i+1} *are defined at the sampling instants* $\left\{t^i_j \mid j \in \mathbb{N}, i \in \{1,2\}\right\}$ *as*

$$\begin{aligned} \xi_{i,\delta_i+1} = \max\left\{\theta_{i,1}|v_i|^2, \varphi_i^2, \gamma_i \phi_i\left((\delta_i+1)h_i\right)\left|\Theta_{i,\delta_i+1} - v_i\right|^2\right\} \\ + \eta_{i,\delta_i+1} - \max\left\{\theta_{i,1}|v_i|^2, \varphi_i^2, \gamma_i \phi_i\left(\delta_i h_i\right)\left|\Theta_{i,\delta_i+1} - v_i\right|^2\right\}. \end{aligned} \tag{41}$$

The resulting coupling constraint between the parameters of dynamic PETQM is given by

$$\left(\frac{\gamma_i}{\phi_i\left(\mathcal{T}^i_{\mathrm{MATI}}\right)} + \theta_{i,1}\right)\theta_{i,1} \le \epsilon_i, \ \frac{\gamma_i}{2\phi_i\left(\mathcal{T}^i_{\mathrm{MATI}}\right)} \le c_i, \ \aleph_i \le \sqrt{\frac{\lambda_i}{\gamma_i}} \min\left\{\ell^2_{i,in}\theta_{i,1}, 1\right\}. \tag{42}$$

Furthermore, let the controller matrices A_c, B_c *and* C_c *be given by* (25). *Then, the closed-loop system described by* (12) - (13) *and* (38) - (39) *is* $\mathcal{L}_2$*-stable with an* $\mathcal{L}_2$*-gain less than or equal to* θ.

Proof. The proof follows a similar approach to that of Theorem 1, in which the Lyapunov function is shown to satisfy properties **a)**, **b)** and **c)**. To characterize the effect of dynamic quantization on the stability of the closed-loop system, we aug-

ment the Lyapunov function with quantization-related terms and define the resulting Lyapunov function candidate as

$$\tilde{U}(t)=V(x)+\sum_{i=1}^{2}\left(\max\left\{\theta_{i,1}|v_i|^2,\varphi_i^2,\gamma_i\phi_i(\delta_i h_i+\tau_i)|e_i|^2\right\}+\eta_{i,\delta_i+1}\right), \tag{43}$$

where $V(x)=x^{\mathrm{T}}Px$ with $P>0$, $\max\left\{\theta_{i,1}|v_i|^2,\varphi_i^2\right\}$ represents the quantization-related term, $\theta_{i,1}>0$, and γ_i satisfy (16) - (17). For ease of subsequent analysis, we define $\tilde{U}_i(t)=\max\left\{\theta_{i,1}|v_i|^2,\varphi_i^2,\gamma_i\phi_i(\delta_i h_i+\tau_i)|e_i|^2\right\}+\eta_{i,\delta_i+1}$.

Property **a)** is trivially satisfied; hence, only properties **b)** and **c)** need to be verified.

Proof of b): For all $t\in\left\{t_j^i \mid j\in\mathbb{N}, i\in\{1,2\}\right\}$, we distinguish the following cases according to the transmission status.

If the triggering condition is not satisfied at a sampling instant, *i.e.*, $t\in\left\{t_j^i \mid j\in\mathbb{N}\right\}\setminus\left\{s_k^i \mid k\in\mathbb{T}_i\right\}$, then $\xi_{i,\delta_i+1}>0$ for all $\delta_i\in\Delta_i$. It then follows from (13) that

$$\begin{aligned}\tilde{U}_i(t^+)-\tilde{U}_i(t)=&\max\left\{\theta_{i,1}|v_i|^2,\varphi_i^2,\gamma_i\phi_i(\delta_i h_i)|e_i|^2\right\}+\eta_{i,\delta_i+1}^+\\&-\left(\max\left\{\theta_{i,1}|v_i|^2,\varphi_i^2,\gamma_i\phi_i(\delta_i h_i+h_i)|e_i|^2\right\}+\eta_{i,\delta_i+1}\right).\end{aligned}$$

By the definition of the triggering function in (41) and $e_i=\Theta_{i,\delta_i+1}-v_i$, we obtain $\tilde{U}_i(t^+)-\tilde{U}_i(t)\le 0$. Since the remaining terms in $\tilde{U}(t)$ do not change at this sampling instant, we consequently obtain $\tilde{U}(t^+)-\tilde{U}(t)\le 0$.

If the triggering condition is satisfied at a sampling instant but packet is lost, *i.e.*, $t\in\left\{s_k^i \mid k\in\mathbb{T}_i\right\}\setminus\left\{z_r^i \mid r\in\mathbb{S}_i\right\}$, it follows from (38) that $\eta_{i,\delta_i+2}^+=\eta_{i,\delta_i+1}$, with the jump updates given by $e_i(t^+)=e_i(t)$, $\delta_i^+=\delta_i+1$ and $\tau_i^+=0$ (with $\tau_i=h_i$). Consequently,

$$\begin{aligned}\tilde{U}_i(t^+)-\tilde{U}_i(t)=&\max\left\{\theta_{i,1}|v_i|^2,\varphi_i^2,\gamma_i\phi_i((\delta_i+1)h_i)|e_i|^2\right\}+\eta_{i,\delta_i+2}^+\\&-\left(\max\left\{\theta_{i,1}|v_i|^2,\varphi_i^2,\gamma_i\phi_i(\delta_i h_i+h_i)|e_i|^2\right\}+\eta_{i,\delta_i+1}\right)\\=&\,0.\end{aligned}$$

Since $V(x)$ and $\tilde{U}_j(t)$, $j\neq i$, remain unchanged at this jump instant, we consequently have $\tilde{U}(t^+)-\tilde{U}(t)=0$

For the successful triggered instants, *i.e.*, $t\in\left\{z_r^i \mid r\in\mathbb{S}_i\right\}$, it follows from (39) that $e_i(t^+)=e_{q,i}(t)$, $\delta_i^+=0$ and $\tau_i^+=0$ (with $\tau_i=h_i$). Accordingly,

$$\tilde{U}_i(t^+)=\max\left\{\theta_{i,1}|v_i|^2,\varphi_i^2,\gamma_i\phi_i(0)|e_{q,i}|^2\right\}+\eta_{i,1}^+.$$

From (40) and the definition of register Θ_i, we have

$$\eta_{i,1}^+\le\bar{\zeta}_i=\max\left\{\theta_{i,1}|v_i|^2,\varphi_i^2,\gamma_i\phi_i((\delta_i+1)h_i)|e_i|^2\right\}+\eta_{i,\delta_i+1}-\max\left\{\theta_{i,1}|v_i|^2,\varphi_i^2\right\}. \tag{44}$$

Next, we consider four cases to verify property **b)** at successful triggered instants.

1) If $\theta_{i,1}|v_i|^2\ge\max\left\{\varphi_i^2,\gamma_i\phi_i(0)|e_{q,i}|^2\right\}$, it follows that

$$\tilde{U}_i\left(t^+\right)-\tilde{U}_i\left(t\right)=\theta_{i,1}\left|v_i\right|^2+\eta_{i,1}^+-\max\left\{\theta_{i,1}\left|v_i\right|^2,\varphi_i^2,\gamma_i\phi_i\left(\left(\delta_i+1\right)h_i\right)\left|e_i\right|^2\right\}-\eta_{i,\delta_i+1}$$
$$\leq 0$$

where the last inequality follows from $\theta_{i,1}\left|v_i\right|^2\leq\max\left\{\theta_{i,1}\left|v_i\right|^2,\varphi_i^2\right\}$.

2) If $\varphi_i^2\geq\max\left\{\theta_{i,1}\left|v_i\right|^2,\gamma_i\phi_i\left(0\right)\left|e_{q,i}\right|^2\right\}$, then $\tilde{U}_i\left(t^+\right)-\tilde{U}_i\left(t\right)\leq 0$.

3) If $\gamma_i\phi_i\left(0\right)\left|e_{q,i}\right|^2\geq\max\left\{\theta_{i,1}\left|v_i\right|^2,\varphi_i^2\right\}$, it follows that

$$\tilde{U}_i\left(t^+\right)-\tilde{U}_i\left(t\right)=\gamma_i\phi_i\left(0\right)\left|e_{q,i}\right|^2+\eta_{i,1}^+-\max\left\{\theta_{i,1}\left|v_i\right|^2,\varphi_i^2,\gamma_i\phi_i\left(\left(\delta_i+1\right)h_i\right)\left|e_i\right|^2\right\}-\eta_{i,\delta_i+1}$$
$$\leq\gamma_i\phi_i\left(0\right)\left|e_{q,i}\right|^2-\max\left\{\theta_{i,1}\left|v_i\right|^2,\varphi_i^2\right\}.$$

By (6) and (37), we have $\left|e_{q,i}\right|^2\leq\aleph_i^2\mu_i^2\leq\aleph_i^2\max\left\{\frac{\left|v_i\right|^2}{\ell_{i,in}^2},\varphi_i^2\right\}$. Since $\phi_i\left(0\right)=\lambda_i^{-1}$ and $\aleph_i^2\leq\frac{\lambda_i}{\gamma_i}\min\left\{\ell_{i,in}^2\theta_{i,1},1\right\}$, it follows that $\tilde{U}_i\left(t^+\right)-\tilde{U}_i\left(t\right)\leq 0$.

4) If $\varphi_i^2=\theta_{i,1}\left|v_i\right|^2=\gamma_i\phi_i\left(0\right)\left|e_{q,i}\right|^2$, then $\tilde{U}_i\left(t^+\right)-\tilde{U}_i\left(t\right)\leq 0$ follows from Lemma II.1 of [32].

Consequently, at successful triggered instant, we have $\tilde{U}\left(t^+\right)-\tilde{U}\left(t\right)\leq 0$.

Hence, property **b)** holds at all jump instants.

Proof of c): We now verify that property **c)** holds for $\tilde{U}\left(t\right)$ during $t\in\mathbb{R}_{\geq 0}\setminus\left\{t_j^i\mid j\in\mathbb{N},i\in\left\{1,2\right\}\right\}$. Due to the maximum term in the Lyapunov function, we consider the following four cases.

i) If $\theta_{i,1}\left|v_i\right|^2>\max\left\{\varphi_i^2,\gamma_i\phi_i\left(\delta_ih_i+\tau_i\right)\left|e_i\right|^2\right\}$, combining (42) with $\phi_i\left(\mathcal{T}_{\mathrm{MATI}}^i\right)\leq\phi_i\left(\delta_ih_i+\tau_i\right)$, yields $\gamma_i^2\left|e_i\right|^2\leq\frac{\gamma_i\theta_{i,1}}{\phi_i\left(\delta_ih_i+\tau_i\right)}\left|v_i\right|^2\leq\left(\epsilon_i-\theta_{i,1}^2\right)\left|v_i\right|^2$. From (11), it gets

$$\frac{\mathrm{d}}{\mathrm{d}t}\left(\theta_{i,1}\left|v_i\right|^2\right)\leq 2\theta_{i,1}\left|v_i\right|\left|\dot{e}_i\right|$$
$$\leq\theta_{i,1}^2\left|v_i\right|^2+\left(A_{e,i}x+B_{e,i}e+E_{e,i}\omega\right)^{\mathrm{T}}\left(A_{e,i}x+B_{e,i}e+E_{e,i}\omega\right).$$

Thus, we can obtain that

$$\tilde{U}_i^\circ\left(q;\frac{\mathrm{d}}{\mathrm{d}t}q\right)+\gamma_i^2\left|e_i\right|^2-\varrho_i\left|v_i\right|^2-\left(A_{e,i}x+B_{e,i}e+E_{e,i}\omega\right)^{\mathrm{T}}\left(A_{e,i}x+B_{e,i}e+E_{e,i}\omega\right)$$
$$\leq\left(\epsilon_i-\varrho_i\right)\left|v_i\right|^2+\Upsilon_{i,\delta_i+1}.$$

ii) If $\varphi_i^2>\max\left\{\theta_{i,1}\left|v_i\right|^2,\gamma_i\phi_i\left(\delta_ih_i+\tau_i\right)\left|e_i\right|^2\right\}$, it follows that $\varphi_i^2\geq\gamma_i\phi_i\left(\mathcal{T}_{\mathrm{MATI}}^i\right)\left|e_i\right|^2$. From $\frac{\gamma_i}{2\phi_i\left(\mathcal{T}_{\mathrm{MATI}}^i\right)}\leq c_i$ in (42), we can obtain that

$$\tilde{U}_i^\circ\left(q;\frac{\mathrm{d}}{\mathrm{d}t}q\right)+\gamma_i^2\left|e_i\right|^2-\varrho_i\left|v_i\right|^2-\left(A_{e,i}x+B_{e,i}e+E_{e,i}\omega\right)^{\mathrm{T}}\left(A_{e,i}x+B_{e,i}e+E_{e,i}\omega\right)$$
$$\leq-2c_i\varphi_i^2+\frac{\gamma_i\varphi_i^2}{\phi_i\left(\mathcal{T}_{\mathrm{MATI}}^i\right)}+\Upsilon_{i,\delta_i+1}-\varrho_i\left|v_i\right|^2$$

$$\le -\varrho_i |v_i|^2 + \Upsilon_{i,\delta_i+1}.$$

iii) If $\gamma_i \phi_i (\delta_i h_i + \tau_i)|e_i|^2 > \max\{\theta_{i,1}|v_i|^2, \varphi_i^2\}$,

$$\begin{aligned}
&\tilde{U}_i^{\circ}\left(q; \frac{\mathrm{d}}{\mathrm{d}t} q\right) + \gamma_i^2 |e_i|^2 - \varrho_i |v_i|^2 - \left(A_{e,i}x + B_{e,i}e + E_{e,i}\omega\right)^{\mathrm{T}} \left(A_{e,i}x + B_{e,i}e + E_{e,i}\omega\right) \\
&\le -\gamma_i \left(\gamma_i \left(\phi_i^2 (\delta_i h_i + \tau_i) + 1\right)\right)|e_i|^2 + 2\gamma_i \phi_i (\delta_i h_i + \tau_i)|e_i| \left|A_{e,i}x + B_{e,i}e + E_{e,i}\omega\right| \\
&\quad + \Upsilon_{i,\delta_i+1} + \gamma_i^2 |e_i|^2 - \varrho_i |v_i|^2 - \left(A_{e,i}x + B_{e,i}e + E_{e,i}\omega\right)^{\mathrm{T}} \left(A_{e,i}x + B_{e,i}e + E_{e,i}\omega\right) \\
&\le -\varrho_i |v_i|^2 + \Upsilon_{i,\delta_i+1}.
\end{aligned}$$

iv) If $\gamma_i \phi_i (\delta_i h_i + \tau_i)|e_i|^2 = \theta_{i,1}|v_i|^2 = \varphi_i^2$, then, by Lemma II.1 of [32], it is known that

$$\begin{aligned}
&\tilde{U}_i^{\circ}\left(q; \frac{\mathrm{d}}{\mathrm{d}t} q\right) + \gamma_i^2 |e_i|^2 - \varrho_i |v_i|^2 - \left(A_{e,i}x + B_{e,i}e + E_{e,i}\omega\right)^{\mathrm{T}} \left(A_{e,i}x + B_{e,i}e + E_{e,i}\omega\right) \\
&\le (\epsilon_i - \varrho_i)|v_i|^2 + \Upsilon_{i,\delta_i+1}.
\end{aligned}$$

Therefore, from $\Upsilon_{i,\delta_i+1} = (\varrho_i - \epsilon_i)|v_i|^2$ and Lemma 1, it follows that property **c)** holds for $\tilde{U}(t)$ during $t \in \mathbb{R}_{\ge 0} \setminus \{t_j^i \mid j \in \mathbb{N}, i \in \{1,2\}\}$.

□

To demonstrate how a dynamic PETQM updates operate without knowing the packet reception results, we provide a compact no-ACK implementation algorithm (**Algorithm 1**). In this framework, it is crucial to distinguish between physically implemented variables and analysis-only states.

Remark 5. *From the above stability analysis, y and u remain bounded for bounded $x(0)$, $e(0)$, $\eta(0)$ and $\omega \in \mathcal{L}_2$. So there exist positive constants $\bar{v}_i$ such that $|v_i| \le \bar{v}_i$. By* (32) *and* (33), *the zoom variable satisfies* $\mu_i \le \bar{\mu}_i = \max\left\{\frac{|\bar{v}_i|}{\ell_{i,in}}, \varphi_i(0), \mu_i(0)\right\}$. *Further,* (34) *and* (35) *yield*

$$0 \le z_{i,in} \le \frac{\log(\varphi_i/\bar{\mu}_i)}{\log \Omega_{i,in}} < \infty \quad \text{and} \quad 0 \le z_{i,out} \le \frac{\log\left(\bar{v}_i/\ell_i \underline{\mu}_i\right)}{\log \Omega_{i,out}}.$$

5. Simulation

To demonstrate the effectiveness of the proposed approach, we consider a benchmark example of a linearized batch reactor, which is adapted from the examples reported in [10]. The plant matrices are given by

$$A_p = \begin{bmatrix} 1.3800 & -0.2077 & 6.7150 & -5.6760 \\ -0.5814 & -4.2900 & 0 & 0.6750 \\ 1.0670 & 4.2730 & -6.6540 & 5.8930 \\ 0.0480 & 4.2730 & 1.3430 & -2.1040 \end{bmatrix}, \quad B_p = \begin{bmatrix} 0 & 0 \\ 5.6790 & 0 \\ 1.1360 & -3.1460 \\ 1.1360 & 0 \end{bmatrix},$$

$$C_p = \begin{bmatrix} 1 & 0 & 1 & -1 \\ 0 & 1 & 0 & 0 \end{bmatrix}, \quad E_p = \begin{bmatrix} 1 & 0 & 1 & 0 \end{bmatrix}^{\mathrm{T}}, \quad C_{zp} = \begin{bmatrix} 0.1 & 0 & 0 & 0 \end{bmatrix}.$$

Solving (16) and (17), we obtain

$$A_c = \begin{bmatrix} -11.8993 & -8.7701 & 36.6199 & 40.8943 \\ -1.6714 & -5.0641 & 3.8434 & 4.0695 \\ -6.1476 & -10.7971 & 29.6418 & 40.2751 \\ 3.4521 & 8.2373 & -21.6322 & -31.0181 \end{bmatrix},$$

$$B_c = \begin{bmatrix} 55.5522 & 24.9476 \\ 9.9006 & 5.1211 \\ 51.1121 & 33.4232 \\ -36.5069 & -25.0197 \end{bmatrix}, \quad C_c = \begin{bmatrix} 0.1100 & 0.0719 & -0.5799 & -0.6038 \\ 0.2690 & -0.0225 & -0.0027 & 0.1812 \end{bmatrix},$$

$$\beta_1 = \beta_2 = 0.2, \ \gamma_1 = \gamma_2 = 20.292.$$

Algorithm 1. Compact no-ACK implementation of dynamic PETQM (node i).

Require: Sampling period h_i, maximum dropouts δ_{max}^i.

Analysis-only States (Unknown to nodes): True successive losses $\delta_i(t)$, internal clock variables $\tau_i(t)$.

— **ENCODER-SIDE (Sensor/Controller)** —

Local Variables: Register Θ_i, dynamic variables η_i, zoom variable μ_i^{enc}.

for each sampling instant $t = t_j^i$ **do**

  Sample current signal $v_i(t_j^i)$.

  Calculate triggering functions ξ_{i,ι_i+1} for all $\iota_i \in \{0, 1, \ldots, \delta_{max}^i\}$ using current η_i and Θ_i.

  if $\min_{\iota_i \in \Delta_i} \xi_{i,\iota_i+1} \leq 0$ **then**

    % Triggering occurs

    Compute integer codes $z_{i,in}$ and $z_{i,out}$ via (34)-(35).

    Update local zoom scale μ_i^{enc} via (32).

    Quantize signal to obtain $v_{q,i}$.

    % Shift local candidate arrays assuming no-ACK

    Update register: $\Theta_i \leftarrow (v_{q,i}, \Theta_{i,1}, \ldots, \Theta_{i,\delta_{max}^i})$ via (38) -(39).

    Transmit packet: $pkt = \{v_{q,i}, z_{i,in}, z_{i,out}\}$.

  else

    % No triggering

    Update dynamic variable η_i via (13).

  end if

end for

— **DECODER-SIDE (Controller/Actuator)** —

Local Variables: Held signal $\hat{v}_{q,i}$, zoom variable μ_i^{dec}.

for any time t **do**

  if a new packet pkt is successfully received **then**

    % Implicitly implies δ_i resets to 0 in analysis

    Extract $v_{q,i}$, $z_{i,in}$, and $z_{i,out}$ from pkt.

    Synchronize zoom scale: update μ_i^{dec} using $z_{i,in}$ and $z_{i,out}$.

    Update held signal: $\hat{v}_{q,i} \leftarrow v_{q,i}$.

  end if

  Apply $\hat{v}_{q,i}$ continuously until the next successful reception.

end for

For the baseline NCS, we set $\lambda_i = 0.6$, $\delta_{\max}^i = 2$ for all $i \in \{1,2\}$. By substituting these parameters into (21), we get $\mathcal{T}_i = 0.0241$ s, $T_i = 0.008$ s and $\varrho_i = 5$ ($i \in \{1,2\}$). Then, we run simulation for 14 s with $x_p(0) = [0.8, -1, 0, 0.5]^{\mathrm{T}}$, $e(0) = 0$, and the external disturbance $\omega(t) = \mathrm{e}^{-t}\sin(2t)$. The state curves are depicted in Figure 2, the triggered instants are described in Figure 3. The numbers of triggered times in the two different networks are 333 and 353, and the numbers of packet losses in these networks are 130 and 125, respectively.

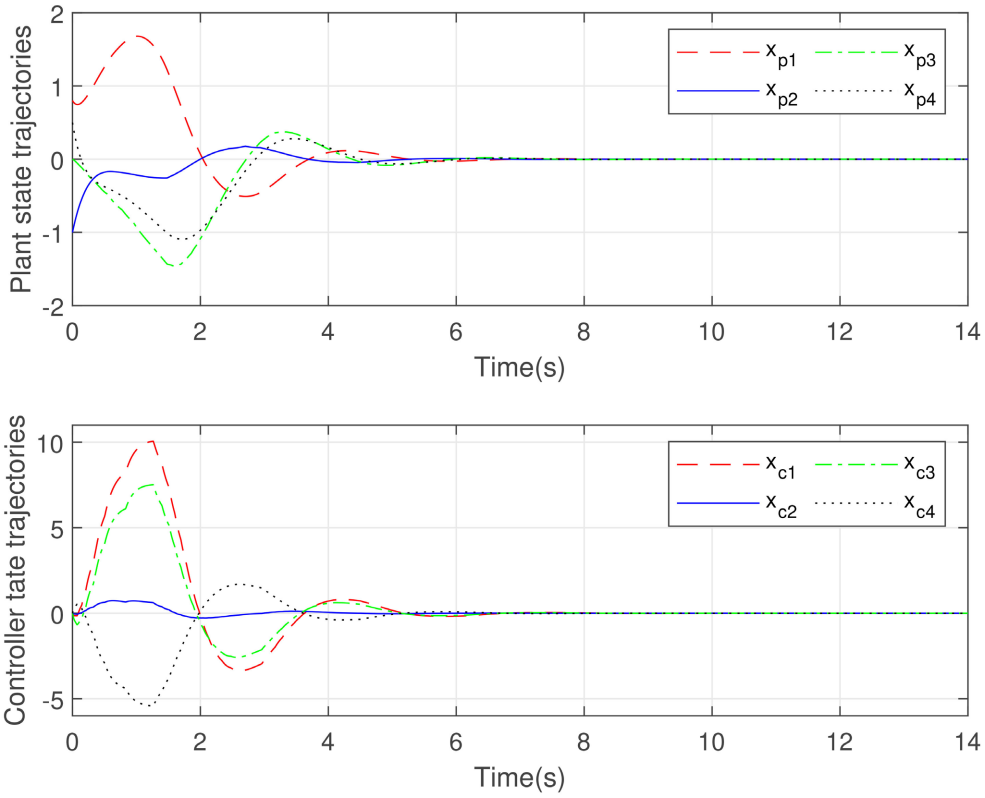

Figure 2. State trajectories of the closed-loop system under the PETM.

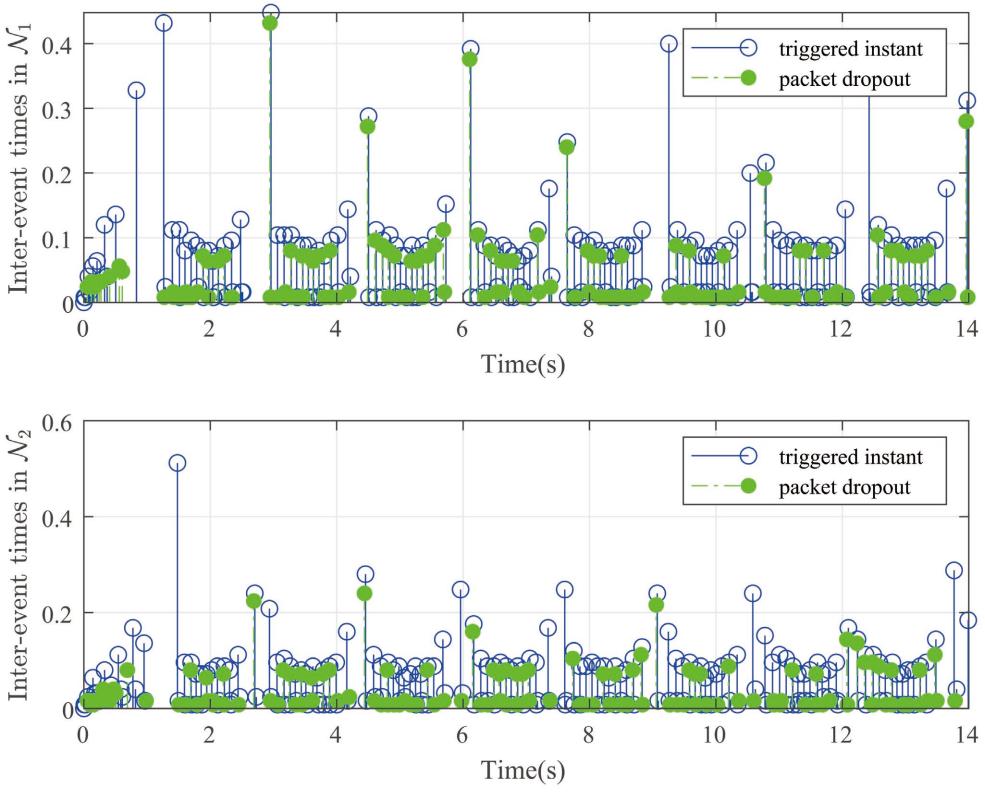

Figure 3. The triggered times in N_1 and N_2 under the PETM with packet losses.

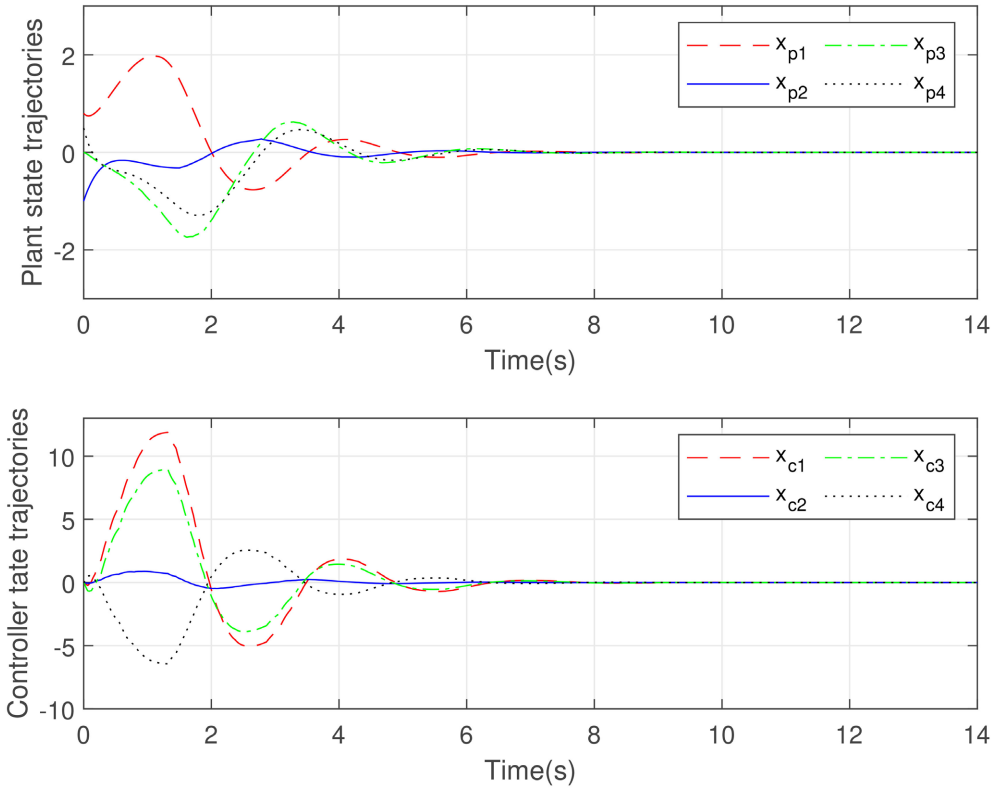

Figure 4. State trajectories of the closed-loop system under the PETQM.

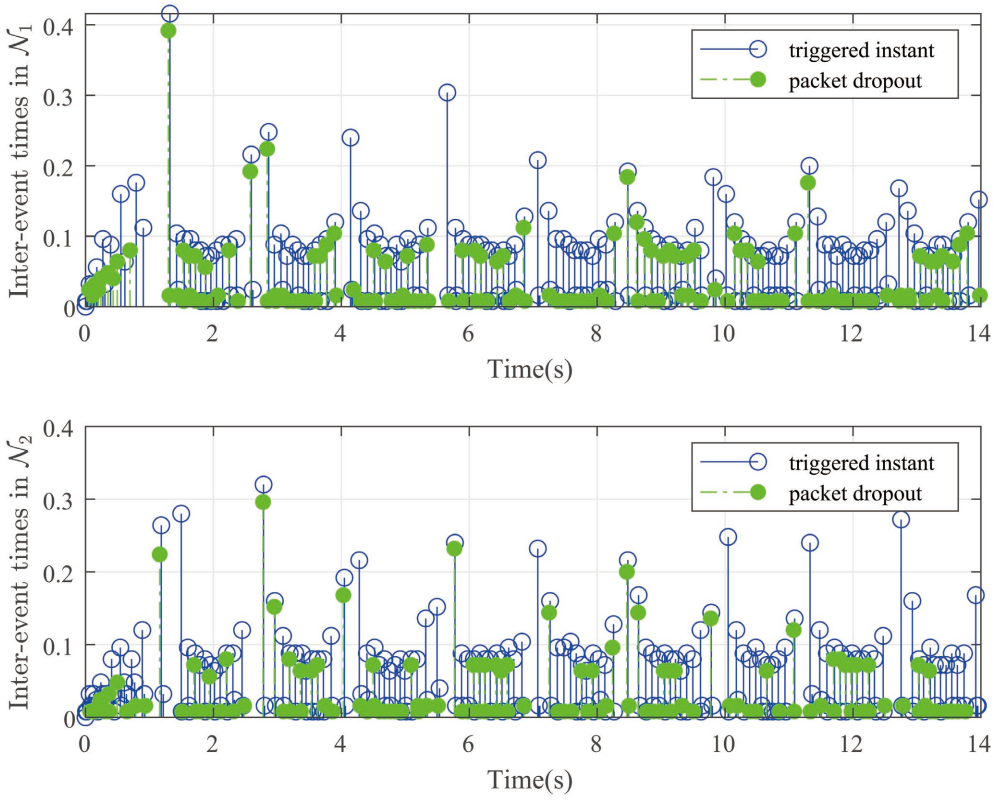

Figure 5. The triggered times in N_1 and N_2 under the PETQM with packet losses.

Based on the theoretical construction in (21), the maximum possible elapsed time without a successful control update under the worst-case packet loss scenario is $\left(\delta_{\max}^{i}+1\right)h_i = 3\times 0.008 = 0.024$ s. Since this calculated worst-case interval strictly satisfies 0.024 s < 0.0241 s = $\mathcal{T}_i$, the chosen sampling periods and the packet loss bounds jointly satisfy the analytical constraints required for dynamic triggering. This guarantees that the closed-loop system maintains $\mathcal{L}_2$-stability despite the simultaneous presence of discrete event-triggering and bounded network losses.

For the proposed NCS, we set $\lambda_i = 0.6$, $\theta_{i,1} = 0.01$ and $\ell_{i,in} = 20$ for all $i \in \{1,2\}$. Substituting these parameters into (42) yields $c_i = 20$, $\aleph_i = 0.1$ and $\epsilon_i = 0.5$. We then choose $M_i = 100$, $\ell_i = 40$, $\ell_{i,out} = 90$ to satisfy (33). The state curves are depicted in **Figure 4**, the triggered instants are described in **Figure 5**. The numbers of triggered times in the two different networks are 366 and 370, and the numbers of packet losses in these networks are 142 and 130, respectively. The average inter-event times in the two networks are 0.0383 s and 0.0378 s, respectively, representing increases of approximately 45.6% and 43.7% over the 0.0263 s value reported in the example of [10].

6. Conclusion

For the baseline NCS with packet losses only, the dynamic PETM accommodates consecutive packet losses by using the information maintained in the network registers and auxiliary dynamic variables. The Lyapunov-based analysis provides sufficient conditions for $\mathcal{L}_2$-stability, based on which the dynamic PETM and dynamic output feedback controller are co-designed. The resulting design compensates for the effects of consecutive packet losses while ensuring $\mathcal{L}_2$-stability and excluding Zeno behavior during signal transmission. The framework was further extended to the case where quantized signals are transmitted over the communication channels. The proposed dynamic quantization scheme adaptively adjusts the quantization scaling parameter according to the transmitted signal and the available quantization range, thereby avoiding quantizer saturation under external disturbances. By integrating the dynamic PETM with the dynamic quantizer, the dynamic PETQM provides a unified treatment of event-triggered transmission, consecutive packet losses, and quantization errors. The resulting stability conditions capture the coupled effects of these communication imperfections and enable the joint determination of the PETQM and dynamic output feedback controller. Numerical examples confirmed that the proposed approach can reduce network transmissions while preserving closed-loop $\mathcal{L}_2$-stability and control performance. Future work will investigate the extension of the proposed framework to NCSs with more general communication constraints, including time-varying delays and scheduling protocols.

Conflicts of Interest

The author declares no conflicts of interest regarding the publication of this paper.

References

[1] Lian, F.L., Moyne, J.R. and Tilbury, D.M. (2000) Control Performance Study of a Networked Machining Cell. *Proceedings of the* 2000 *American Control Conference. ACC* (IEEE Cat. No. 00CH36334), **42**, 2337-2341. https://doi.org/10.1109/acc.2000.878598

[2] Hassine, E., Thabet, A., Gasmi, N. and Bel Haj Frej, G. (2025) An Event-Triggered Observer-Based Control Approach for Enhancing Resilience of Cyber-Physical Systems under Markovian Cyberattacks. *Actuators*, **14**, Article 412. https://doi.org/10.3390/act14080412

[3] Pezzutto, M., Dey, S., Garone, E., Gatsis, K., Johansson, K.H. and Schenato, L. (2024) Wireless Control: Retrospective and Open Vistas. *Annual Reviews in Control*, **58**, Article 100972. https://doi.org/10.1016/j.arcontrol.2024.100972

[4] Wei, Z.-J., Du, X., Liu, K.-Z. and Sun, X.-M. (2024) Data-Driven Dynamic Event-Triggered Control for NCSS under Denial-of-Service and Time-Varying Delays. *IEEE Transactions on Intelligent Transportation Systems*, **25**, 11156-11167. https://doi.org/10.1109/tits.2024.3370945

[5] Qu, F.R., Liu, Z.W., Liu, X.K., Wang, Y.W. and Tian, E. G. (2024) Memory-Based Event-Triggered Control for Distributed Secondary Control in DC Microgrids with Quantized Communication. *IEEE Transactions on Industrial Electronics*, **71**, 14864-14874. https://doi.org/10.1109/tie.2024.3376793

[6] Tabuada, P. (2007) Event-Triggered Real-Time Scheduling of Stabilizing Control Tasks. *IEEE Transactions on Automatic Control*, **52**, 1680-1685. https://doi.org/10.1109/tac.2007.904277

[7] Wu, Y.B., Guo, Z.R., Xue, L., Ahn, C.K. and Liu, J. (2024) Stabilization of Complex Networks under Asynchronously Intermittent Event-Triggered Control. *Automatica*, **161**, Article 111493. https://doi.org/10.1016/j.automatica.2023.111493

[8] Zhang, X.M., Han, Q.L., Ge, X.H., Ding, D.R., Ning, B.D. and Zhang, B.L. (2025) An Overview of Recent Advances in Event-Triggered Control. *Science China Information Sciences*, **68**, Article No. 161201. https://doi.org/10.1007/s11432-024-4437-9

[9] Dolk, V. and Heemels, M. (2017) Event-Triggered Control Systems under Packet Losses. *Automatica*, **80**, 143-155. https://doi.org/10.1016/j.automatica.2017.02.029

[10] Wu, C., Zhao, X., Xia, W., Liu, J. and Başar, T. (2021) L_2 -Gain Analysis for Dynamic Event-Triggered Networked Control Systems with Packet Losses and Quantization. *Automatica*, **129**, Article 109587. https://doi.org/10.1016/j.automatica.2021.109587

[11] Heemels, W.P.M.H., Donkers, M.C.F. and Teel, A.R. (2011) Periodic Event-Triggered Control Based on State Feedback. *IEEE Conference on Decision and Control and European Control Conference*, Orlando, 12-15 December 2011, 2571-2576. https://doi.org/10.1109/cdc.2011.6160817

[12] Girard, A. (2015) Dynamic Triggering Mechanisms for Event-Triggered Control. *IEEE Transactions on Automatic Control*, **60**, 1992-1997. https://doi.org/10.1109/tac.2014.2366855

[13] Borgers, D.P., Dolk, V.S. and Heemels, M.W.P.M.H. (2017) Dynamic Periodic Event-Triggered Control for Linear Systems. *Proceedings of the* 20*th International Conference on Hybrid Systems: Computation and Control*, Pittsburgh, 18-20 April 2017, 179-186. https://doi.org/10.1145/3049797.3049815

[14] Hertneck, M., Linsenmayer, S. and Allgower, F. (2019) Nonlinear Dynamic Periodic Event-Triggered Control with Robustness to Packet Loss Based on Non-Monotonic Lyapunov Functions. 2019 *IEEE* 58*th Conference on Decision and Control* (*CDC*), Nice, 11-13 December 2019, 1680-1685.

https://doi.org/10.1109/cdc40024.2019.9029770

[15] Li, C.C., Xu, F.D., Wang, Y.H. and Zhao, X.D. (2024) Data-Driven Dynamic Periodic Event-Triggered Control of Cyber-Physical Systems under Packet Dropouts and DoS Attacks. *IEEE Transactions on Information Forensics and Security*, **19**, 7187-7199. https://doi.org/10.1109/tifs.2024.3431280

[16] Zhu, X.L., Zhang, X.X., Wei, J.M., Wen, C.Y. and Lin, H. (2026) Periodic Event-Triggered Quantized Control for Nonlinear Systems with Packet Losses and Large Transmission Delays. *IEEE Transactions on Automatic Control*, **71**, 3926-3941. https://doi.org/10.1109/tac.2026.3653601

[17] Yu, Q.X., Fan, Z.H., Bu, X.H. and Hou, Z.S. (2024) Event-Triggered Based Predictive Iterative Learning Control with Random Packet Loss Compensation for Nonlinear Networked Systems. *ISA Transactions*, **148**, 169-181. https://doi.org/10.1016/j.isatra.2024.03.001

[18] Kooshkbaghi, M. and Marquez, H.J. (2020) Event-Triggered Discrete-Time Cubature Kalman Filter for Nonlinear Dynamical Systems with Packet Dropout. *IEEE Transactions on Automatic Control*, **65**, 2278-2285. https://doi.org/10.1109/tac.2019.2945286

[19] Dolk, V.S. and Heemels, W.P.M.H. (2015) Dynamic Event-Triggered Control under Packet Losses: The Case with Acknowledgements. 2015 *International Conference on Event-Based Control, Communication, and Signal Processing* (EBCCSP), Krakow, 17-19 June 2015, 1-7. https://doi.org/10.1109/ebccsp.2015.7300651

[20] Garcia, E. and Antsaklis, P.J. (2013) Model-Based Event-Triggered Control for Systems with Quantization and Time-Varying Network Delays. *IEEE Transactions on Automatic Control*, **58**, 422-434. https://doi.org/10.1109/tac.2012.2211411

[21] El Chamie, M., Liu, J. and Basar, T. (2016) Design and Analysis of Distributed Averaging with Quantized Communication. *IEEE Transactions on Automatic Control*, **61**, 3870-3884. https://doi.org/10.1109/tac.2016.2530939

[22] Liberzon, D. (2003) Hybrid Feedback Stabilization of Systems with Quantized Signals. *Automatica*, **39**, 1543-1554. https://doi.org/10.1016/s0005-1098(03)00151-1

[23] Abdelrahim, M., Dolk, V.S. and Heemels, W.P.M.H. (2019) Event-Triggered Quantized Control for Input-to-State Stabilization of Linear Systems with Distributed Output Sensors. *IEEE Transactions on Automatic Control*, **64**, 4952-4967. https://doi.org/10.1109/tac.2019.2900338

[24] Wu, C.Y., Zhao, X.D., Zong, G.D. and Liu, L.J. (2025) Dynamic Periodic Event-Triggered Control for Networked Control Systems with Dynamic Quantization and Time-Varying Delays. *IEEE Internet of Things Journal*, **12**, 34102-34112. https://doi.org/10.1109/jiot.2025.3578507

[25] Ren, Y.W., Cai, P.T., Fang, Y.X. and Niu, B. (2025) Dynamic Quantized Event-Triggered Predictive Control for Networked Control Systems with DoS Attacks: A Hybrid System Approach. *IEEE Transactions on Signal and Information Processing over Networks*, **11**, 1138-1150. https://doi.org/10.1109/tsipn.2025.3606196

[26] Shan, Y., Xie, X.P., Sun, J.Y. and Park, J.H. (2024) Observer-Based Adaptive Event-Triggered Control for Nonlinear Networked Systems under Multiple Cyber Attacks. *IEEE Transactions on Fuzzy Systems*, **32**, 5272-5284. https://doi.org/10.1109/tfuzz.2024.3418953

[27] Lei, Y.F., Li, J.M. and Lu, X.J. (2026) Spatial Decentralized Dynamic Event-Triggered Quantized Control for Semilinear Parabolic Systems. *IEEE Internet of Things Journal*, **13**, 3360-3370. https://doi.org/10.1109/jiot.2025.3634081

[28] Coutinho, P.H.S., Pessim, P.S.P., Bessa, I., Peixoto, M.L.D.C. and Palhares, R.M. (2026)

Handling Asynchronous Scheduling Functions in Periodic Event-Triggered Gain-Scheduled Control with Guaranteed Polytopic Inclusion. *IEEE Transactions on Cybernetics*, **56**, 4206-4218. https://doi.org/10.1109/tcyb.2026.3671185

[29] Ban, J., Seo, M., Goh, T., Jeong, H. and Kim, S.W. (2020) Improved Co-Design of Event-Triggered Dynamic Output Feedback Controllers for Linear Systems. *Automatica*, **111**, Article 108600. https://doi.org/10.1016/j.automatica.2019.108600

[30] Dolk, V.S., Borgers, D.P. and Heemels, W.P.M.H. (2017) Output-Based and Decentralized Dynamic Event-Triggered Control with Guaranteed $\mathcal{L}_p$ -Gain Performance and ZeNo-Freeness. *IEEE Transactions on Automatic Control*, **62**, 34-49. https://doi.org/10.1109/tac.2016.2536707

[31] Carnevale, D., Teel, A.R. and Nesic, D. (2007) A Lyapunov Proof of an Improved Maximum Allowable Transfer Interval for Networked Control Systems. *IEEE Transactions on Automatic Control*, **52**, 892-897. https://doi.org/10.1109/tac.2007.895913

[32] Liberzon, D., Nesic, D. and Teel, A.R. (2014) Lyapunov-Based Small-Gain Theorems for Hybrid Systems. *IEEE Transactions on Automatic Control*, **59**, 1395-1410. https://doi.org/10.1109/tac.2014.2304397